scientific reports

Check for updates

OPEN

Gramicidin S and melittin: potential anti-viral therapeutic peptides to treat SARS-CoV-2 infection

Mohammed Ghalib Enayathullah[1,2], Yash Parekh[1,2], Sarena Banu[1], Sushma Ram[1], Ramakrishnan Nagaraj[1], Bokara Kiran Kumar[1]✉ & Mohammed M. Idris[1]✉

The COVID19 pandemic has led to multipronged approaches for treatment of the disease. Since de novo discovery of drugs is time consuming, repurposing of molecules is now considered as one of the alternative strategies to treat COVID19. Antibacterial peptides are being recognized as attractive candidates for repurposing to treat viral infections. In this study, we describe the anti-SARS-CoV-2 activity of the well-studied antibacterial peptides gramicidin S and melittin obtained from *Bacillus brevis* and bee venom respectively. The EC_{50} values for gramicidin S and melittin were 1.571 µg and 0.656 µg respectively based on in vitro antiviral assay. Significant decrease in the viral load as compared to the untreated group with no/very less cytotoxicity was observed. Both the peptides treated to the SARS-CoV-2 infected Vero cells showed viral clearance from 12 h onwards with a maximal viral clearance after 24 h post infection. Proteomics analysis indicated that more than 250 proteins were differentially regulated in the gramicidin S and melittin treated SARS-CoV-2 infected Vero cells against control SARS-CoV-2 infected Vero cells after 24 and 48 h post infection. The identified proteins were found to be associated in the metabolic and mRNA processing of the Vero cells post-treatment and infection. Both these peptides could be attractive candidates for repurposing to treat SARS-CoV-2 infection.

The pandemic caused by SARS-CoV-2 has led to intense research not only on the biology of the virus but also therapeutic interventions with a multi-pronged approach[1]. Vaccines have been developed at "warp" speed. The overall efficacies of different vaccines, though variable are excellent[2] and have played a major role in controlling the disease[3]. However, vaccines are not available universally and there have been cases of infection with SARS-CoV-2 even in vaccinated individuals, though not severe[4]. Also, the effect of vaccines would wane over time. The vaccines may also be less effective against newly emerging strains such as omicron which has a very large number of substitutions in the viral genome as compared to the earlier strains (https://www.cdc.gov/coronavirus/2019-ncov/science/science-briefs/scientific-brief-omicron-variant.html). There is clearly a need for development of therapeutic agents in addition to vaccines. In the area of anti-infective agents against SARS-CoV-2, efforts have been taken to generate therapeutic antibodies that would neutralize the virus and prevent its interaction with cellular receptors to gain entry into cells[5]. Considering the time scales in developing a drug de novo, there have been several attempts to re-purpose drugs to treat COVID19[1,6,7]. However, repurposed drugs have had very limited success in treating SARS-CoV-2 infection including remdesivir[8]. There is no drug to-date that can be used specifically to treat COVID19 disease. Although two drugs from Pfizer (Paxlovid) and Merck (Molnupiravir) appear to show promise, their effectiveness is still to be established unequivocally[9].

Infection in the case of SARS-CoV-2 is initiated by binding of the spike protein to ACE2 followed by a series of steps leading to fusion and internalization of the virus and propagation[1,10]. If the binding of the spike protein to ACE2 is prevented, then the virus will no longer be able to enter cells and propagate. SARS-CoV-2 is an enveloped virus where the RNA is encapsulated within a lipid vesicular structure with the spike protein decorating on the external side giving the "corona" appearance[1,10]. Disruption of the lipid structure would lead to the disintegration of the virus. Naturally occurring membrane-active peptides have potent antimicrobial activity which stems from their ability to disrupt bacterial membranes[11,12]. We have explored the antiviral activity of two extensively studied peptides, gramicidin S having the sequence: [cyclo-(Val-Orn-Leu-D-Phe-Pro)2][13] and the bee venom peptide, melittin having the sequence: GIGAVLKVLTTGLPALISWIKRKRQQ-amide[14]. We reasoned that if the peptides could destabilize the viral membrane, the virus would disintegrate and would thus be rendered inactive. The peptides could also conceivably bind to the spike protein and prevents its interaction with ACE2 or inhibit fusion.

[1]CSIR-Centre for Cellular and Molecular Biology, Hyderabad, Telangana 500007, India. [2]These authors contributed equally: Mohammed Ghalib Enayathullah and Yash Parekh. ✉email: bokarakiran@ccmb.res.in; idris@ccmb.res.in

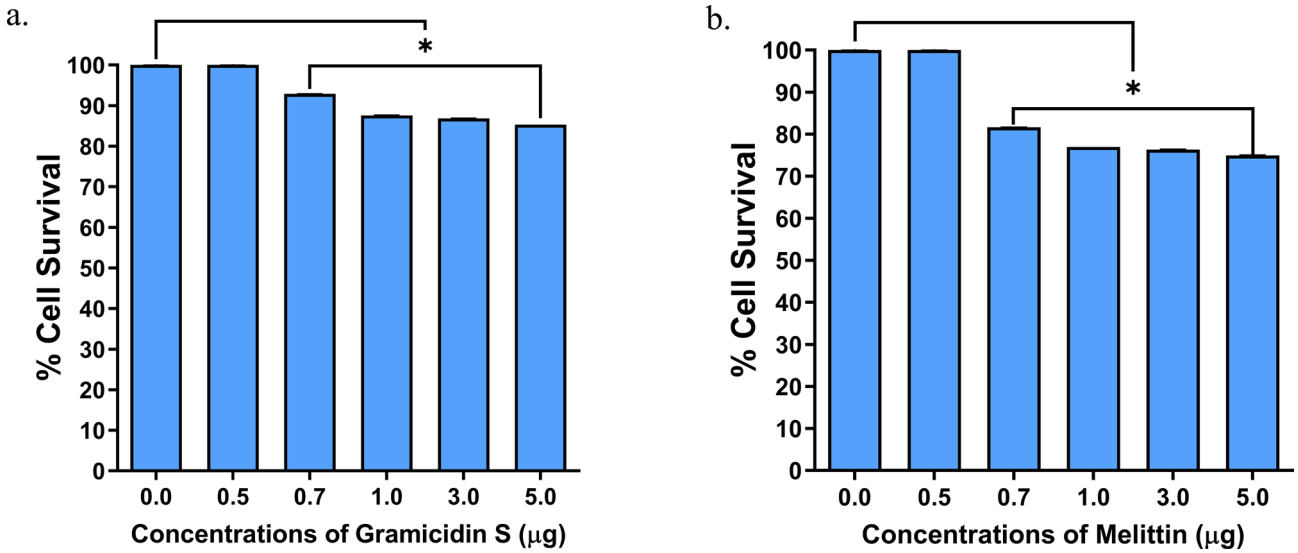

Figure 1. Measurement of Cytolytic activity of gramicidin S and melittin using MTT Assay: The graphs represent the percentage of cell viability vs. concentrations of (**a**) Gramicidin S (μg). (**b**) Melittin (μg). The values represent Mean ± SD of atleast three independent experiments. The data analysis and graphs were generated using GraphPad Prism (*Ver* 8.4.2). Significance of variance, $p < 0.05$ is considered statistically significant.

Peptides are crucial components of host-defense against bacteria and fungi in species across the evolutionary scale[11,12]. There has been intense research in recent years to examine whether these and related peptides have the ability to neutralize SARS-CoV-2 and also have therapeutic potential[12,15–17]. They include naturally occurring peptides that can be easily isolated. Many of these peptides have also been investigated structurally. These include gramicidin S and the bee venom peptide melittin[13,14]. The antiviral activity of melittin against several viruses has been investigated extensively[18]. Nano-conjugates of melittin with sitagliptin have been investigated for anti-SARS-CoV-2 activity[19]. Other pharmacological activities of melittin have also been investigated[20,21]. Gramicidin S has been used therapeutically to treat dental applications in humans[22].

The antiviral activity of melittin has been reported previously. Hood et al., reported that melittin is highly effective in reducing HIV-1 infectivity[23]. Uddin et al., reported antiviral effect of melittin on different viruses (VSV-GFP, HSV-GFP, EV71, H3-GFP, RSV-GFP) both in vitro and in vivo[24]. Several studies showed melittin is effective against diverse array of viruses such as coxsackievirus, enterovirus, influenza A viruses, human immunodeficiency virus (HIV), herpes simplex virus (HSV), Junín virus (JV), respiratory syncytial virus (RSV), vesicular stomatitis virus (VSV), and tobacco mosaic virus (TMV)[18]. Not much scientific evidences or reports are available so far for the antiviral activity of the gramicidin S. Gramicidin S showed cell cytotoxicity (CC50) at 18.7 μg/ml in HT-29 cells[25]. Melittin showed CC50 of 6.45 μg/ml in C654 cells[26].

We have investigated the antiviral activity of gramicidin S and melittin against SARS-CoV-2 in vitro in detail. We have observed that both the peptides have the ability to neutralize the virus in an in vitro assay using Vero cells. At the EC_{50} value, there is no cytolytic activity. The viral load had decreased drastically in the treatment group as seen by confocal microscopic images. Proteomic analysis indicates that there is also a metabolic effect and not merely viral lysis. Both the peptides could be attractive candidates for development as therapeutic agents to treat SARS-CoV-2 infection. As the viral membrane would be a likely target, mutant strains may also be susceptible to the peptides.

Results

Antiviral activity of peptides. The cytolytic activity of gramicidin S and melittin was determined using MTT assay (Fig. 1). Results showed 75–80% cell survival at all the concentrations tested (up to 5 μg) indicating the safe use of these peptides (Fig. 1). The SARS-CoV-2 viral particles enumerated by the RT-qPCR showed that treatment of gramicidin S and melittin effectively reduced viral load in vitro Log EC_{50} value of gramicidin S (0.1963) corresponds to 1.571 μg and Log EC_{50} value (2.826) of melittin corresponds to 0.656 μg (Fig. 2) The antiviral activity of gramicidin S (3.0 μg) and melittin (1.5 μg) at 12 and 24 h was examined along with remdesivir (1 μM) as assay control. The data shown in Fig. 3 indicates that the peptides show antiviral activity at 12 h and is more pronounced at 24 h. The gramicidin S and melittin showed 99% and 95% viral reduction respectively at 12 h compared with remdesivir (20%). At 24 h remdesivir showed 90% viral reduction whereas both gramicidin S and melittin showed 99% viral reduction. The SARS-CoV-2 antiviral activity of gramicidin S and melittin was compared with remdesivir by confocal microscopy (Fig. 4). Panel B (green fluorescence) indicates infection of cells, more prominent at 24 h. Panels D and E correspond to virus incubated with gramicidin S and melittin before incubating with cells. The considerable decrease in green fluorescence indicates that both the peptides have good anti-viral activity as with remdesivir shown in Panel E. Although, antiviral activity is observed at 12 h, it is more pronounced at 24 h.

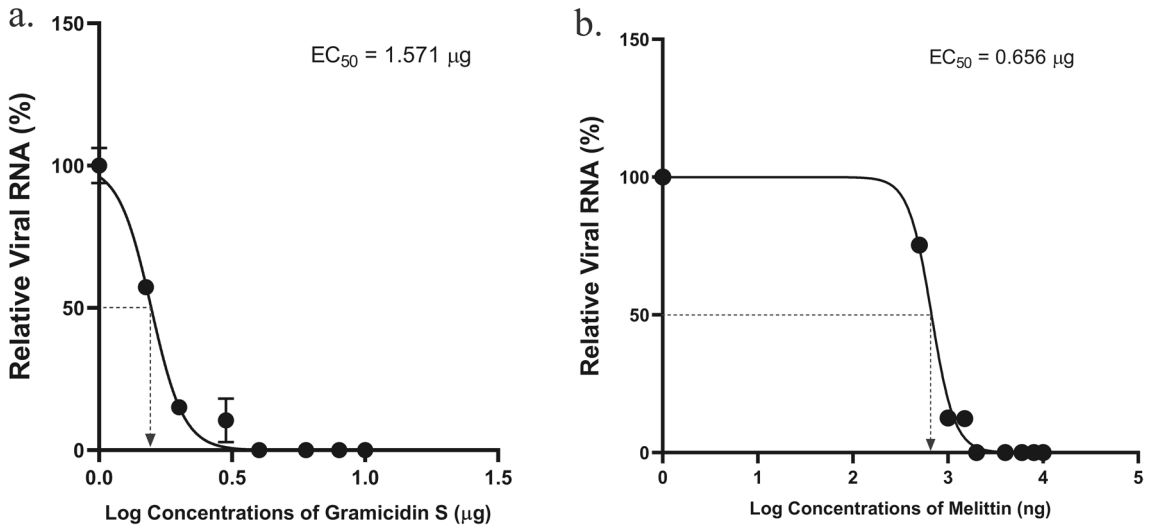

Figure 2. Anti SARS-CoV-2 activity of gramicidin S and melittin in vitro: (**a**). Relative viral RNA (%) vs. Log concentrations of gramicidin S (µg). (**b**) Relative viral RNA (%) vs. Log concentrations of melittin (ng). The graphs represent the Ct values of N-gene calculated using RT-qPCR in the supernatants. The Log EC_{50} value of gramicidin S (0.1963) corresponds to 1.571 µg and Log EC_{50} value (2.826) of melittin corresponds to 0.656 µg as shown in the graph.

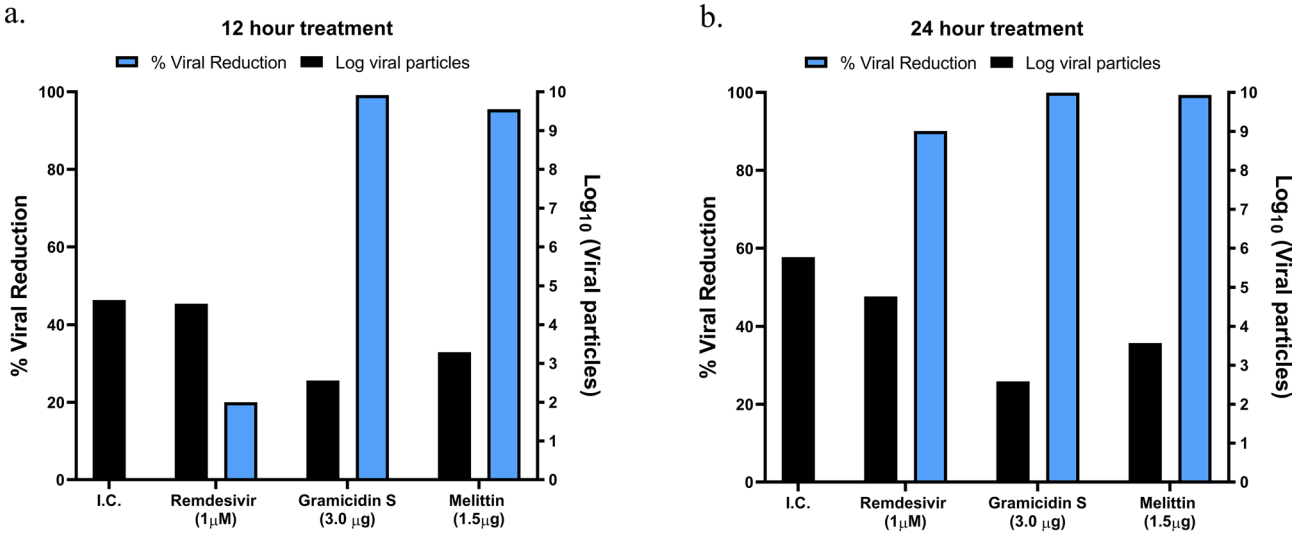

Figure 3. The anti SARS-CoV2 activity of remdesivir gramicidin S and melittin at 12 (**a**) and 24 (**b**) h post infection. The X axis represents different experimental groups: I.C (infection control), remdesivir (1 µM), gramicidin S (3.0 µg), and melittin (1.5 µg). The Y axis (Blue bars) represents % of viral reduction and Y'-Axis (black bars) represents the Log_{10} viral particles.

Proteomic analysis. The effect of the peptides on the ability of virus to infect Vero cells was studied by high-throughput proteomic analysis. iTRAQ based quantitative proteomics analysis identified 7 SARS-CoV-2 proteins as up regulated in the control infected Vero Cells. Nsp9, ORF1ab, ORF10 and nucleocapsid phosphoprotein were found to be up-regulated in the Vero cells after 24 h of infection, whereas the same proteins were found to be down regulated in the cells upon gramicidin S and melittin treatment (Table 1). Similarly, at 48 h post infection (hpi), ORF1ab, S protein, nucleocapsid phosphoprotein, helicase and RNA-dependent RNA polymerase were found to be up-regulated in the infected Vero cells which were found to be down regulated in the gramicidin S and melittin treated Vero cells (Table 1).

Based on proteomics analysis, a total of 254 proteins were found to be differentially regulated and associated in infected and peptide treated Vero cells (Table 2 and Fig. 5a). It was found that majority of up and down regulated proteins were reversed with gramicidin S and melittin treatment at 24 and 48 hpi. RS28, K22E, K2C1, RL17 are few of the major down-regulated proteins which were found to be reversing their expression post peptide treatment. NPM, ACLY, CALX and F184B were found to be up-regulated in Vero cells after 24hpi, whereas peptide treatment showed reversal of the protein expression (Table 2). Heat map analysis showed that gramicidin S and melittin-treated cells at their respective time point post infection are rooted together against out rooting with

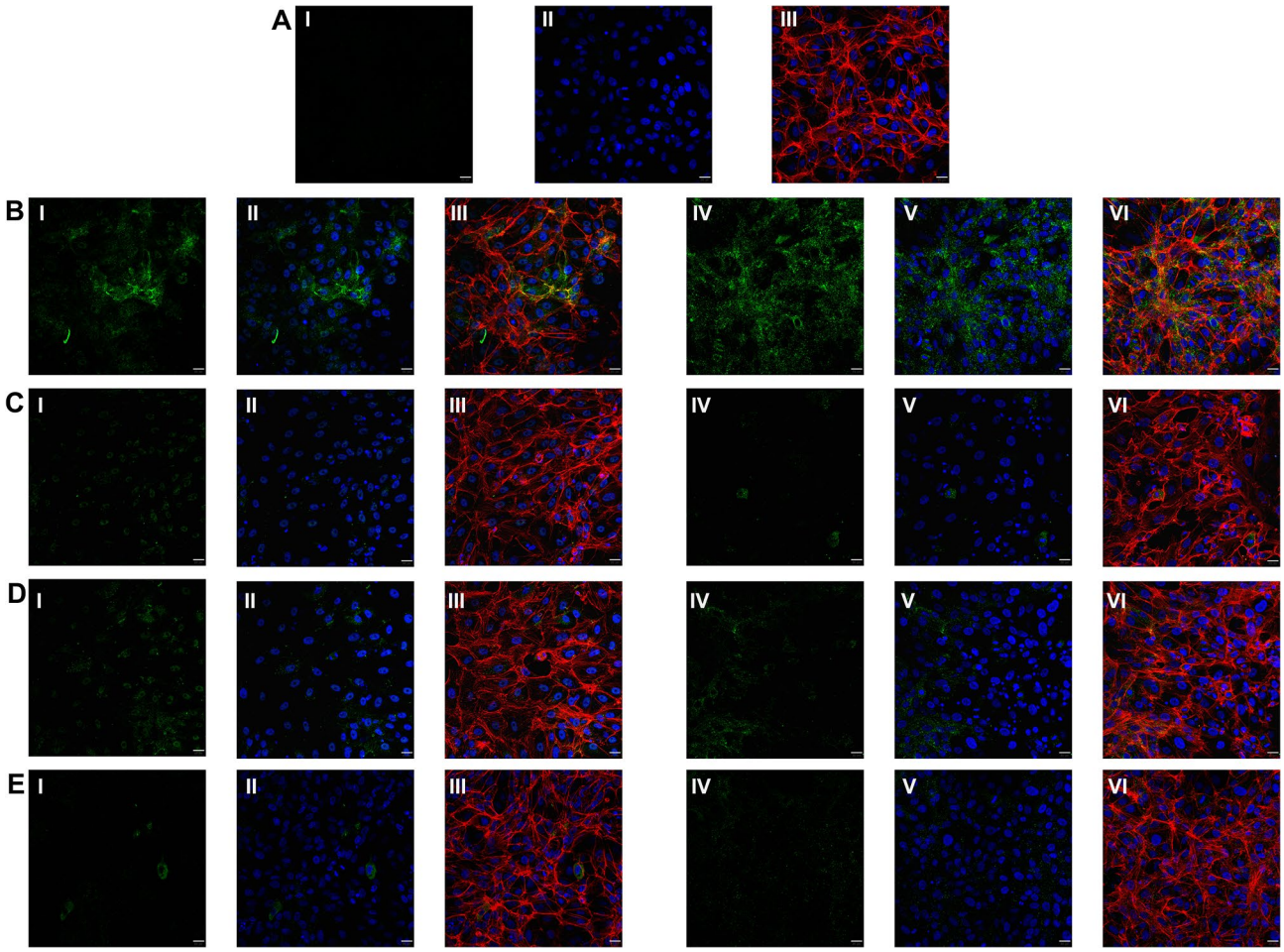

Figure 4. Immunofluorescence staining images against RBD protein expression specific to SARS-CoV-2 in Vero cells. (**A**) (I) Vero cells without SARS-CoV-2 infection (mock), (II) DAPI staining representing nucleus (blue); (III) Merged image of f-Actin (Phalloidin staining, red), nucleus (DAPI, blue). (**B**) Vero cells infected with SARS-CoV-2, (I) represents RBD protein expression (green) of SARS-CoV-2 virus at 12 h; (II) DAPI staining representing nucleus (blue) along with RBD protein expression of SARS-CoV-2 (green) at 12 h; (III) Merged image of f-Actin (red) (Phalloidin staining), nucleus (DAPI) and RBD protein of SARS-CoV-2 (green) at 12 h; (IV) represents RBD protein expression (green) of SARS-CoV-2 virus at 24 h; (V) DAPI staining representing nucleus (blue) along with RBD protein expression of SARS-CoV-2 (green) at 24 h; (VI) Merged image of f-Actin (Phalloidin staining, red), nucleus (DAPI, blue) and RBD protein of SARS-CoV-2 (green) at 24 h. (**C**) Vero cells infected with SARS-CoV-2 treated with gramicidin S, (I) RBD protein expression (green) of SARS-CoV-2 virus at 12 h; (II) DAPI staining representing nucleus (blue) along with RBD protein expression of SARS-CoV-2 (green) at 12 h; (III) Merged image of f-Actin (red) (Phalloidin staining), nucleus (DAPI) and RBD protein of SARS-CoV-2 (green) at 12 h; (IV) represents RBD protein expression (green) of SARS-CoV-2 virus at 24 h; (V) DAPI staining representing nucleus (blue) along with RBD protein expression of SARS-CoV-2 (green) at 24 h; (VI) Merged image f-Actin (Phalloidin staining, red), nucleus (DAPI, blue) and RBD protein of SARS-CoV-2 (green) at 24 h. (**D**) Vero cells infected with SARS-CoV-2 treated with melittin. (I) represents RBD protein expression (green) of SARS-CoV-2 virus at 12 h; (II) DAPI staining representing nucleus (blue) along with RBD protein expression of SARS-CoV-2 (green) at 12 h; (III) Merged image of f-Actin (red) (Phalloidin staining), nucleus (DAPI) and RBD protein of SARS-CoV-2 (green) at 12 h; (IV) represents RBD protein expression (green) of SARS-CoV-2 virus at 24 h; (V) DAPI staining representing nucleus (blue) along with RBD protein expression of SARS-CoV-2 (green) at 24 h; (VI) Merged image of f-Actin (Phalloidin staining, red), nucleus (DAPI, blue) and RBD protein of SARS-CoV-2 (green) at 24 h. (**E**) Vero cells infected with SARS-CoV-2 treated with remdesivir, (I) represents RBD protein expression (green) of SARS-CoV-2 virus at 12 h; (II) DAPI staining representing nucleus (blue) along with RBD protein expression of SARS-CoV-2 (green) at 12 h; (III) Merged image of f-Actin (red) (Phalloidin staining), nucleus (DAPI) and RBD protein of SARS-CoV-2 (green) at 12 h; (IV) represents RBD protein expression (green) of SARS-CoV-2 virus at 24 h; (V) DAPI staining representing nucleus (blue) along with RBD protein expression of SARS-CoV-2 (green)at 24 h; (VI) Merged image of f-Actin (Phalloidin staining, red), nucleus (DAPI, blue) and RBD protein of SARS-CoV-2 (green) at 24 h. Scale bars, 20 μm (40 × image).

Time Point	Protein Accession No.	Protein Name	# Peptides	# PSMs	Infected Controls	Gramicidin S treated Infected cells	Melittin treated Infected cells
24hpi	YP_009742616.1	nsp9 [Severe acute respiratory syndrome coronavirus 2]	17	69	0.1	–1.2	–0.9
	YP_009724389.1	ORF1ab polyprotein [Severe acute respiratory syndrome coronavirus 2]	762	3246	0.3	–1.3	–1.1
	YP_009725255.1	ORF10 protein [Severe acute respiratory syndrome coronavirus 2]	4	9	0.5	–1.2	–1.4
	YP_009724397.2	nucleocapsid phosphoprotein [Severe acute respiratory syndrome coronavirus 2]	71	260	0.6	0.1	1.6
48hpi	YP_009724389.1	ORF1ab polyprotein [Severe acute respiratory syndrome coronavirus 2]	755	3587	0.8	–0.8	–0.9
	YP_009724390.1	surface glycoprotein [Severe acute respiratory syndrome coronavirus 2]	108	418	0.1	–1.3	–0.7
	YP_009724397.2	nucleocapsid phosphoprotein [Severe acute respiratory syndrome coronavirus 2]	75	271	2.2	–2.8	–2.7
	YP_009725308.1	helicase [Severe acute respiratory syndrome coronavirus 2]	83	312	0.2	–1.2	–0.3
	YP_009725307.1	RNA-dependent RNA polymerase [Severe acute respiratory syndrome coronavirus 2]	106	492	0.9	–1.0	–1.6

Table 1. List of SARS-CoV-2 proteins and their expression level in the vero cells post infection (control), gramicidin S treatment and melittin treatment.

infected cells for the same time point post infection. It is very interesting to see the tight association of peptide treated Vero cell protein expression against control infected Vero cell protein expression for both the time points post infection (Fig. 5a).

A total of 125 proteins were selected for the Network and pathway analysis involving STRING v11.5. Based on Gene ontological functional enrichment analysis it was found that cellular process (125 proteins), biological regulation (108 proteins) and regulation of biological process (104 proteins) are the most highly associated biological processes; binding (113 proteins), proteins binding (87 proteins) and heterocyclic compound binding (84 proteins) are the most associated molecular functions and cellular anatomical entity (129 proteins), intracellular (125 proteins) and organelle (122 proteins) are the most occurred cellular components. Carbon metabolism (Blue color nodes), pentose phosphate pathway (Blue color nodes) and mRNA processing (Red color nodes) were most prominent local network cluster associated with STRING analysis (Fig. 5b). G6PD, PGK1, ALDOA, ALDOC, TKT, TALDO, LDHB, LDHA, PGAM1 and PGAM2 were the proteins which were found to be associated with carbon metabolism and pentose phosphate pathway analysis. Similarly TRA2B, RBMX, HNRPM, PTBP1, HNRPK, SRSF1, HNRPU, DDX5 and HNRPC proteins were found to be associated with mRNA processing pathway.

Interaction of gramicidin S and melittin with RBD domain of spike protein: In silico analysis. Both gramicidin S and melittin are membrane-active peptides and exert their antimicrobial activity by interacting with membrane components[13,14]. Both the peptides may exert their antiviral activity by targeting multiple regions of the virus. The ability of the peptides to bind to the receptor binding domain (RBD) of the SARS-CoV-2 spike protein was examined by molecular docking using web version of the program ZDOCK[27]. The structures shown in Fig. 6 indicate that both gramicidin S and melittin can bind to the RBD binding domain. Both the structures were in the top ten predictions in the ZDOCK output. Panel A shows the crystal structure of RBD-ACE2 complex. The interface between RBD and ACE are shown in violet color and stick representation respectively. The models of gramicidin S and melittin are shown in panels B and C respectively. The LigPlot[28] of the interacting amino acids are shown in panels D for gramicidin S and E for melittin. The residues highlighted in yellow are involved in RBD binding to ACE2[10]. The modeling study indicates that both the peptides can bind to RBD although their sequences are considerably different from the RBD binding region of ACE2. Both the peptides did not dock to the N-terminal region of ACE2 that binds to RBD region of the spike protein in the top 10 predictions (data not shown).

Discussion

During the past two decades, the world had witnessed infection by three highly pathogenic human corona viruses namely, SARS-Co-V, MERS, SARS-CoV-2[29,30]. They belong to the group of β-coronavirus and have the ability to cross animal-human barriers and cause serious illness in humans. The timely development of specific antivirals is of utmost importance.The development of vaccines at "warp speed" has led to decrease in mortality and serious illness caused by SARS-CoV-2[3]. However, it is still not well established that whether vaccines are equally effective against the several variants that are emerging, such as the omicron variant, or the time frame when immunity will be present. To-date, there is no specific drug for SARS-CoV-2. Hence, there is clearly an urgent need to develop therapeutic molecules that would effectively neutralize the virus rather than repurposing drugs used to treat

UNIPROT ID	Description	Symbol	# Peptides	# PSMs	24 hours post infection (hpi)			48 hours post infection (hpi)		
					Infected controls	Gramicidin S treated Infected cells	Melittin treated Infected cells	Infected controls	Gramicidin S treated Infected cells	Melittin treated Infected cells
O14744	Protein arginine N-methyltransferase 5 OS=Homo sapiens OX=9606 GN=PRMT5 PE=1 SV=4 - [ANM5_HUMAN]	ANM5	7	9	0.1	−1.4	−0.9	−0.9	−0.9	0.7
O14818	Proteasome subunit alpha type-7 OS=Homo sapiens OX=9606 GN=PSMA7 PE=1 SV=1 - [PSA7_HUMAN]	PSA7	5	7	−0.3	−1.8	−0.7	0.2	−0.1	0.1
O14979	Heterogeneous nuclear ribonucleoprotein D-like OS=Homo sapiens OX=9606 GN=HNRNPDL PE=1 SV=3 - [HNRDL_HUMAN]	HNRDL	6	9	0.4	−1.8	−1.0	0.1	−1.5	0.2
O43175	D-3-phosphoglycerate dehydrogenase OS=Homo sapiens OX=9606 GN=PHGDH PE=1 SV=4 - [SERA_HUMAN]	SERA	5	6	−0.4	−1.0	−0.3	1.0	−0.3	−1.2
O60218	Aldo-keto reductase family 1 member B10 OS=Homo sapiens OX=9606 GN=AKR1B10 PE=1 SV=2 - [AK1BA_HUMAN]	AK1BA	6	7	1.4	−0.8	1.5	−0.9	−0.2	0.2
O60318	Germinal-center associated nuclear protein OS=Homo sapiens OX=9606 GN=MCM3AP PE=1 SV=2 - [GANP_HUMAN]	GANP	16	18	−0.4	−1.0	−0.3	0.1	−1.6	0.0
O60701	UDP-glucose 6-dehydrogenase OS=Homo sapiens OX=9606 GN=UGDH PE=1 SV=1 - [UGDH_HUMAN]	UGDH	8	8	−0.5	−1.3	−0.7	1.6	−0.4	−2.3
O75390	Citrate synthase, mitochondrial OS=Homo sapiens OX=9606 GN=CS PE=1 SV=2 - [CISY_HUMAN]	CISY	8	10	1.4	−0.6	1.4	−1.1	−1.0	−0.7
O95359	Transforming acidic coiled-coil-containing protein 2 OS=Homo sapiens OX=9606 GN=TACC2 PE=1 SV=3 - [TACC2_HUMAN]	TACC2	14	18	−1.0	−1.4	−1.7	1.3	−1.0	−1.5
O95831	Apoptosis-inducing factor 1, mitochondrial OS=Homo sapiens OX=9606 GN=AIFM1 PE=1 SV=1 - [AIFM1_HUMAN]	AIFM1	9	11	0.1	−2.0	−0.9	1.0	−0.6	−1.5
P00338	L-lactate dehydrogenase A chain OS=Homo sapiens OX=9606 GN=LDHA PE=1 SV=2 - [LDHA_HUMAN]	LDHA	14	29	1.3	−1.2	0.7	−1.5	−1.6	−1.7
P00352	Retinal dehydrogenase 1 OS=Homo sapiens OX=9606 GN=ALDH1A1 PE=1 SV=2 - [AL1A1_HUMAN]	AL1A1	5	9	0.3	−1.5	−1.5	−0.4	−1.2	0.0
P00390	Glutathione reductase, mitochondrial OS=Homo sapiens OX=9606 GN=GSR PE=1 SV=2 - [GSHR_HUMAN]	GSHR	7	10	0.2	−1.9	−1.5	−0.6	−0.9	0.3
P00492	Hypoxanthine-guanine phosphoribosyltransferase OS=Homo sapiens OX=9606 GN=HPRT1 PE=1 SV=2 - [HPRT_HUMAN]	HPRT	1	1	0.0	−1.3	−1.0	0.4	−2.3	−0.9
P00505	Aspartate aminotransferase, mitochondrial OS=Homo sapiens OX=9606 GN=GOT2 PE=1 SV=3 - [AATM_HUMAN]	AATM	8	11	1.1	−0.7	1.0	−1.9	−1.8	−1.5
P00558	Phosphoglycerate kinase 1 OS=Homo sapiens OX=9606 GN=PGK1 PE=1 SV=3 - [PGK1_HUMAN]	PGK1	19	33	1.4	−0.7	1.6	−1.6	−1.8	−2.2
P00966	Argininosuccinate synthase OS=Homo sapiens OX=9606 GN=ASS1 PE=1 SV=2 - [ASSY_HUMAN]	ASSY	6	6	0.7	−1.3	0.6	−1.3	−0.3	0.6
P02545	Prelamin-A/C OS=Homo sapiens OX=9606 GN=LMNA PE=1 SV=1 - [LMNA_HUMAN]	LMNA	17	17	−0.9	−1.4	−0.9	1.6	−1.7	−0.5
P02751	Fibronectin OS=Homo sapiens OX=9606 GN=FN1 PE=1 SV=4 - [FINC_HUMAN]	FINC	18	24	−1.2	−1.2	0.6	−0.2	−0.8	−1.3
P02768	Serum albumin OS=Homo sapiens OX=9606 GN=ALB PE=1 SV=2 - [ALBU_HUMAN]	ALBU	9	15	−1.7	1.1	−0.3	0.5	0.5	−1.7
P04075	Fructose-bisphosphate aldolase A OS=Homo sapiens OX=9606 GN=ALDOA PE=1 SV=2 - [ALDOA_HUMAN]	ALDOA	21	36	1.2	−0.6	1.3	−1.7	−1.6	−1.3
P04083	Annexin A1 OS=Homo sapiens OX=9606 GN=ANXA1 PE=1 SV=2 - [ANXA1_HUMAN]	ANXA1	18	36	0.6	−0.4	1.4	−1.4	−1.2	−1.7
P04179	Superoxide dismutase [Mn], mitochondrial OS=Homo sapiens OX=9606 GN=SOD2 PE=1 SV=3 - [SODM_HUMAN]	SOD2	6	12	0.4	0.6	0.7	2.2	−1.1	−1.5
P04264	Keratin, type II cytoskeletal 1 OS=Homo sapiens OX=9606 GN=KRT1 PE=1 SV=6 - [K2C1_HUMAN]	K2C1	32	63	−2.6	0.1	0.5	−0.6	−0.9	−0.7
P04406	Glyceraldehyde-3-phosphate dehydrogenase OS=Homo sapiens OX=9606 GN=GAPDH PE=1 SV=3 - [G3P_HUMAN]	G3P	19	67	1.4	−0.9	1.4	−1.9	−1.5	−1.9
P04792	Heat shock protein beta-1 OS=Homo sapiens OX=9606 GN=HSPB1 PE=1 SV=2 - [HSPB1_HUMAN]	HSPB1	11	21	−1.1	−1.9	−0.6	0.0	−0.2	−0.1
P05121	Plasminogen activator inhibitor 1 OS=Homo sapiens OX=9606 GN=SERPINE1 PE=1 SV=1 - [PAI1_HUMAN]	PAI1	5	6	−0.5	−0.6	−0.1	−0.5	−1.1	0.1
P05141	ADP/ATP translocase 2 OS=Homo sapiens OX=9606 GN=SLC25A5 PE=1 SV=7 - [ADT2_HUMAN]	ADT2	13	22	−0.7	−0.5	−0.6	−0.6	−0.8	0.2
P05386	60S acidic ribosomal protein P1 OS=Homo sapiens OX=9606 GN=RPLP1 PE=1 SV=1 - [RLA1_HUMAN]	RLA1	1	7	−1.9	−1.2	0.9	2.6	−1.8	−2.7
P05388	60S acidic ribosomal protein P0 OS=Homo sapiens OX=9606 GN=RPLP0 PE=1 SV=1 - [RLA0_HUMAN]	RLA0	10	24	1.2	−0.2	1.7	−1.4	−1.6	−2.0
P05783	Keratin, type I cytoskeletal 18 OS=Homo sapiens OX=9606 GN=KRT18 PE=1 SV=2 - [K1C18_HUMAN]	K1C18	15	20	−0.7	−1.3	−0.8	−2.1	−1.2	−1.2
P06576	ATP synthase subunit beta, mitochondrial OS=Homo sapiens OX=9606 GN=ATP5F1B PE=1 SV=3 - [ATPB_HUMAN]	ATPB	11	20	0.3	−1.8	−1.1	1.3	−0.7	−1.6
P06733	Alpha-enolase OS=Homo sapiens OX=9606 GN=ENO1 PE=1 SV=2 - [ENOA_HUMAN]	ENOA	23	45	−0.6	−1.6	−0.4	1.2	−0.5	−1.9
P06744	Glucose-6-phosphate isomerase OS=Homo sapiens OX=9606 GN=GPI PE=1 SV=4 - [G6PI_HUMAN]	G6PI	6	10	−0.1	0.0	1.9	2.0	−1.8	−0.8
P06748	Nucleophosmin OS=Homo sapiens OX=9606 GN=NPM1 PE=1 SV=2 - [NPM_HUMAN]	NPM	18	38	2.2	−1.1	1.5	−2.1	−0.9	−0.8
P06753	Tropomyosin alpha-3 chain OS=Homo sapiens OX=9606 GN=TPM3 PE=1 SV=2 - [TPM3_HUMAN]	TPM3	13	22	1.3	−1.2	0.8	−1.5	−1.0	−1.1

Table 2. (continued)

P07195	L-lactate dehydrogenase B chain OS=Homo sapiens OX=9606 GN=LDHB PE=1 SV=2 - [LDHB_HUMAN]	LDHB	16	22	1.5	−1.1	1.1	−1.9	−1.2	−1.4
P07237	Protein disulfide-isomerase OS=Homo sapiens OX=9606 GN=P4HB PE=1 SV=3 - [PDIA1_HUMAN]	PDIA1	13	17	0.0	0.1	2.7	−0.2	−1.5	0.1
P07305	Histone H1.0 OS=Homo sapiens OX=9606 GN=H1F0 PE=1 SV=3 - [H10_HUMAN]	H10	1	2	0.2	−0.4	−0.4	0.2	−1.8	−0.8
P07355	Annexin A2 OS=Homo sapiens OX=9606 GN=ANXA2 PE=1 SV=2 - [ANXA2_HUMAN]	ANXA2	37	100	1.4	−0.6	1.4	−2.0	−1.2	−1.6
P07437	Tubulin beta chain OS=Homo sapiens OX=9606 GN=TUBB PE=1 SV=2 - [TBB5_HUMAN]	TBB5	21	48	−0.5	−1.8	−0.8	1.3	−0.6	−2.2
P07711	Cathepsin L1 OS=Homo sapiens OX=9606 GN=CTSL PE=1 SV=2 - [CATL1_HUMAN]	CATL1	8	11	−0.2	−1.6	−0.8	−0.1	0.3	0.2
P07737	Profilin-1 OS=Homo sapiens OX=9606 GN=PFN1 PE=1 SV=2 - [PROF1_HUMAN]	PROF1	4	6	0.9	0.7	0.9	2.3	−1.9	−3.1
P07910	Heterogeneous nuclear ribonucleoproteins C1/C2 OS=Homo sapiens OX=9606 GN=HNRNPC PE=1 SV=4 - [HNRPC_HUMAN]	HNRPC	12	18	1.5	−1.1	0.9	−2.1	−1.5	−1.6
P08133	Annexin A6 OS=Homo sapiens OX=9606 GN=ANXA6 PE=1 SV=3 - [ANXA6_HUMAN]	ANXA6	12	14	−0.6	−0.8	−1.1	−0.3	−1.1	0.1
P08238	Heat shock protein HSP 90-beta OS=Homo sapiens OX=9606 GN=HSP90AB1 PE=1 SV=4 - [HS90B_HUMAN]	HS90B	30	60	0.3	−1.4	−1.1	−0.2	0.5	−1.1
P08243	Asparagine synthetase [glutamine-hydrolyzing] OS=Homo sapiens OX=9606 GN=ASNS PE=1 SV=4 - [ASNS_HUMAN]	ASNS	4	4	0.0	−1.9	−0.9	−1.4	−0.3	0.9
P08670	Vimentin OS=Homo sapiens OX=9606 GN=VIM PE=1 SV=4 - [VIME_HUMAN]	VIME	35	65	−0.9	−1.2	−0.7	1.3	−0.5	−1.6
P08758	Annexin A5 OS=Homo sapiens OX=9606 GN=ANXA5 PE=1 SV=2 - [ANXA5_HUMAN]	ANXA5	14	24	−0.6	−0.9	−0.2	−1.2	−1.2	−1.4
P08865	40S ribosomal protein SA OS=Homo sapiens OX=9606 GN=RPSA PE=1 SV=4 - [RSSA_HUMAN]	RSSA	7	14	0.4	0.2	1.5	−1.2	−0.8	−2.8
P09211	Glutathione S-transferase P OS=Homo sapiens OX=9606 GN=GSTP1 PE=1 SV=2 - [GSTP1_HUMAN]	GSTP1	2	2	−2.0	−2.0	0.9	4.7	−2.1	−3.5
P09382	Galectin-1 OS=Homo sapiens OX=9606 GN=LGALS1 PE=1 SV=2 - [LEG1_HUMAN]	LEG1	4	7	−1.8	−0.9	0.7	1.8	−1.9	−2.4
P09525	Annexin A4 OS=Homo sapiens OX=9606 GN=ANXA4 PE=1 SV=4 - [ANXA4_HUMAN]	ANXA4	15	26	0.5	−0.6	1.0	0.5	−1.0	−0.4
P09651	Heterogeneous nuclear ribonucleoprotein A1 OS=Homo sapiens OX=9606 GN=HNRNPA1 PE=1 SV=5 - [ROA1_HUMAN]	ROA1	21	45	−0.7	−2.5	−0.8	−0.1	−0.3	0.2
P09972	Fructose-bisphosphate aldolase C OS=Homo sapiens OX=9606 GN=ALDOC PE=1 SV=2 - [ALDOC_HUMAN]	ALDOC	6	15	−0.4	−1.1	−1.5	−2.1	−1.0	−1.2
P0CG48	Polyubiquitin-C OS=Homo sapiens OX=9606 GN=UBC PE=1 SV=3 - [UBC_HUMAN]	UBC	8	10	1.1	0.2	1.3	2.6	−1.6	−1.9
P10412	Histone H1.4 OS=Homo sapiens OX=9606 GN=HIST1H1E PE=1 SV=2 - [H14_HUMAN]	H14	13	18	1.1	−0.1	1.9	0.5	−1.9	−2.3
P10809	60 kDa heat shock protein, mitochondrial OS=Homo sapiens OX=9606 GN=HSPD1 PE=1 SV=2 - [CH60_HUMAN]	CH60	20	24	−1.0	1.1	3.2	1.2	−0.5	−2.0
P11021	Endoplasmic reticulum chaperone BiP OS=Homo sapiens OX=9606 GN=HSPA5 PE=1 SV=2 - [BIP_HUMAN]	BIP	17	35	−0.8	−0.9	0.1	0.4	−0.2	−0.9
P11142	Heat shock cognate 71 kDa protein OS=Homo sapiens OX=9606 GN=HSPA8 PE=1 SV=1 - [HSP7C_HUMAN]	HSP7C	22	31	−0.1	0.2	2.4	1.6	−1.2	−1.8
P11413	Glucose-6-phosphate 1-dehydrogenase OS=Homo sapiens OX=9606 GN=G6PD PE=1 SV=4 - [G6PD_HUMAN]	G6PD	6	12	0.0	−2.1	−0.9	−2.0	0.4	1.2
P11586	C-1-tetrahydrofolate synthase, cytoplasmic OS=Homo sapiens OX=9606 GN=MTHFD1 PE=1 SV=3 - [C1TC_HUMAN]	C1TC	10	11	0.4	−0.8	−0.9	0.1	0.4	−0.4
P12236	ADP/ATP translocase 3 OS=Homo sapiens OX=9606 GN=SLC25A6 PE=1 SV=4 - [ADT3_HUMAN]	ADT3	5	9	−0.2	−0.8	−1.4	−0.1	0.5	0.2
P13489	Ribonuclease inhibitor OS=Homo sapiens OX=9606 GN=RNH1 PE=1 SV=2 - [RINI_HUMAN]	RINI	3	6	1.6	−1.2	0.8	−1.7	0.0	0.8
P13639	Elongation factor 2 OS=Homo sapiens OX=9606 GN=EEF2 PE=1 SV=4 - [EF2_HUMAN]	EF2	23	35	0.3	−1.3	−1.0	−2.3	1.3	2.4
P13645	Keratin, type I cytoskeletal 10 OS=Homo sapiens OX=9606 GN=KRT10 PE=1 SV=6 - [K1C10_HUMAN]	K1C10	22	41	−0.9	−1.0	−1.0	−0.3	−1.4	−1.1
P13647	Keratin, type II cytoskeletal 5 OS=Homo sapiens OX=9606 GN=KRT5 PE=1 SV=3 - [K2C5_HUMAN]	K2C5	15	17	−0.9	0.1	2.4	1.8	−0.4	−2.4
P13667	Protein disulfide-isomerase A4 OS=Homo sapiens OX=9606 GN=PDIA4 PE=1 SV=2 - [PDIA4_HUMAN]	PDIA4	7	8	0.6	−1.9	−1.4	−0.4	−4.0	−1.1
P14618	Pyruvate kinase PKM OS=Homo sapiens OX=9606 GN=PKM PE=1 SV=4 - [KPYM_HUMAN]	KPYM	28	44	−0.7	0.2	2.3	1.6	−0.8	−2.5
P14625	Endoplasmin OS=Homo sapiens OX=9606 GN=HSP90B1 PE=1 SV=1 - [ENPL_HUMAN]	ENPL	20	31	0.4	−1.4	−1.3	−3.3	−0.9	−1.1
P14868	Aspartate--tRNA ligase, cytoplasmic OS=Homo sapiens OX=9606 GN=DARS PE=1 SV=2 - [SYDC_HUMAN]	SYDC	8	9	0.0	−2.1	−0.7	−1.7	0.1	1.0
P15121	Aldose reductase OS=Homo sapiens OX=9606 GN=AKR1B1 PE=1 SV=3 - [ALDR_HUMAN]	ALDR	14	29	1.3	−1.5	0.6	−2.1	−1.1	−1.2
P15259	Phosphoglycerate mutase 2 OS=Homo sapiens OX=9606 GN=PGAM2 PE=1 SV=3 - [PGAM2_HUMAN]	PGAM2	6	7	0.3	0.6	0.9	0.0	−1.6	−0.7
P15559	NAD(P)H dehydrogenase [quinone] 1 OS=Homo sapiens OX=9606 GN=NQO1 PE=1 SV=1 - [NQO1_HUMAN]	NQO1	3	4	−0.2	−1.4	−1.4	−0.1	0.1	−0.2
P15880	40S ribosomal protein S2 OS=Homo sapiens OX=9606 GN=RPS2 PE=1 SV=2 - [RS2_HUMAN]	RS2	14	17	−0.6	−1.3	−0.3	−0.4	0.4	0.3
P16152	Carbonyl reductase [NADPH] 1 OS=Homo sapiens OX=9606 GN=CBR1 PE=1 SV=3 - [CBR1_HUMAN]	NADPH	8	11	1.2	−0.4	1.7	0.0	0.2	0.1
P17844	Probable ATP-dependent RNA helicase DDX5 OS=Homo sapiens OX=9606 GN=DDX5 PE=1 SV=1 - [DDX5_HUMAN]	DDX5	12	15	−0.9	0.3	2.2	0.4	−1.9	−0.1

Table 2. (continued)

P17987	T-complex protein 1 subunit alpha OS=Homo sapiens OX=9606 GN=TCP1 PE=1 SV=1 - [TCPA_HUMAN]	TCPA	6	7	0.1	−1.8	−1.1	1.4	−2.9	−1.2
P18124	60S ribosomal protein L7 OS=Homo sapiens OX=9606 GN=RPL7 PE=1 SV=1 - [RL7_HUMAN]	RL7	9	11	0.0	0.5	1.3	1.1	−1.8	−1.4
P18621	60S ribosomal protein L17 OS=Homo sapiens OX=9606 GN=RPL17 PE=1 SV=3 - [RL17_HUMAN]	RL17	3	4	−2.0	−1.5	0.3	−2.7	1.7	4.2
P18669	Phosphoglycerate mutase 1 OS=Homo sapiens OX=9606 GN=PGAM1 PE=1 SV=2 - [PGAM1_HUMAN]	PGAM1	6	7	−0.4	−1.5	−1.2	−0.8	0.4	0.7
P19105	Myosin regulatory light chain 12A OS=Homo sapiens OX=9606 GN=MYL12A PE=1 SV=2 - [ML12A_HUMAN]	ML12A	4	8	−0.6	−1.2	−0.2	1.0	−1.0	−1.8
P19338	Nucleolin OS=Homo sapiens OX=9606 GN=NCL PE=1 SV=3 - [NUCL_HUMAN]	NUCL	11	14	0.5	−1.3	−1.1	0.2	0.6	−0.8
P20073	Annexin A7 OS=Homo sapiens OX=9606 GN=ANXA7 PE=1 SV=3 - [ANXA7_HUMAN]	ANXA7	6	7	0.1	−1.6	−1.2	−1.0	−2.1	−1.7
P21291	Cysteine and glycine-rich protein 1 OS=Homo sapiens OX=9606 GN=CSRP1 PE=1 SV=3 - [CSRP1_HUMAN]	CSRP1	5	7	−0.8	−0.9	−0.8	−1.6	0.5	1.1
P21333	Filamin-A OS=Homo sapiens OX=9606 GN=FLNA PE=1 SV=4 - [FLNA_HUMAN]	FLNA	26	38	0.1	−1.0	−0.9	−0.5	1.0	−1.6
P22087	rRNA 2'-O-methyltransferase fibrillarin OS=Homo sapiens OX=9606 GN=FBL PE=1 SV=2 - [FBRL_HUMAN]	FBRL	10	15	1.1	−0.3	1.7	−1.0	−2.1	−2.0
P22392	Nucleoside diphosphate kinase B OS=Homo sapiens OX=9606 GN=NME2 PE=1 SV=1 - [NDKB_HUMAN]	NDKB	6	11	−1.6	−1.2	0.8	1.9	−2.0	−3.0
P22626	Heterogeneous nuclear ribonucleoproteins A2/B1 OS=Homo sapiens OX=9606 GN=HNRNPA2B1 PE=1 SV=2 - [ROA2_HUMAN]	ROA2	12	23	1.0	−1.0	0.8	−1.9	−2.1	−2.7
P23284	Peptidyl-prolyl cis-trans isomerase B OS=Homo sapiens OX=9606 GN=PPIB PE=1 SV=2 - [PPIB_HUMAN]	PPIB	3	6	−0.7	−1.1	−0.5	−1.7	0.7	1.4
P23396	40S ribosomal protein S3 OS=Homo sapiens OX=9606 GN=RPS3 PE=1 SV=2 - [RS3_HUMAN]	RS3	8	10	0.9	0.4	2.1	−1.6	0.2	0.4
P23526	Adenosylhomocysteinase OS=Homo sapiens OX=9606 GN=AHCY PE=1 SV=4 - [SAHH_HUMAN]	SAHH	7	11	0.9	−0.4	1.6	−1.2	−1.5	−1.6
P23528	Cofilin-1 OS=Homo sapiens OX=9606 GN=CFL1 PE=1 SV=3 - [COF1_HUMAN]	COF1	3	6	−1.8	−0.6	0.2	3.2	−1.7	−2.8
P24534	Elongation factor 1-beta OS=Homo sapiens OX=9606 GN=EEF1B2 PE=1 SV=3 - [EF1B_HUMAN]	EF1B	4	6	1.9	−1.1	1.2	−1.7	−1.3	−1.7
P25705	ATP synthase subunit alpha, mitochondrial OS=Homo sapiens OX=9606 GN=ATP5F1A PE=1 SV=1 - [ATPA_HUMAN]	ATPA	14	15	−0.5	0.2	2.2	−0.2	−1.2	0.2
P25786	Proteasome subunit alpha type-1 OS=Homo sapiens OX=9606 GN=PSMA1 PE=1 SV=1 - [PSA1_HUMAN]	PSA1	5	7	1.4	−0.7	1.3	−1.9	−1.2	−1.3
P25788	Proteasome subunit alpha type-3 OS=Homo sapiens OX=9606 GN=PSMA3 PE=1 SV=2 - [PSA3_HUMAN]	PSA3	5	6	−0.6	−1.4	−0.4	−0.9	−0.2	0.5
P26038	Moesin OS=Homo sapiens OX=9606 GN=MSN PE=1 SV=3 - [MOES_HUMAN]	MOES	8	10	0.5	−2.1	−1.3	1.8	−1.9	−0.9
P26373	60S ribosomal protein L13 OS=Homo sapiens OX=9606 GN=RPL13 PE=1 SV=4 - [RL13_HUMAN]	RL13	11	19	−0.9	−1.4	−0.3	−0.5	0.7	0.3
P26599	Polypyrimidine tract-binding protein 1 OS=Homo sapiens OX=9606 GN=PTBP1 PE=1 SV=1 - [PTBP1_HUMAN]	PTBP1	8	13	0.2	−1.7	−1.1	−0.5	−1.1	0.3
P26641	Elongation factor 1-gamma OS=Homo sapiens OX=9606 GN=EEF1G PE=1 SV=3 - [EF1G_HUMAN]	EF1G	9	11	0.2	−1.6	−1.0	−1.2	−0.6	0.9
P27348	14-3-3 protein theta OS=Homo sapiens OX=9606 GN=YWHAQ PE=1 SV=1 - [1433T_HUMAN]	1433T	6	14	−0.3	−0.9	−2.1	1.1	−1.1	−1.2
P27797	Calreticulin OS=Homo sapiens OX=9606 GN=CALR PE=1 SV=1 - [CALR_HUMAN]	CALR	7	8	−0.1	−2.7	−1.0	−1.7	−0.1	0.7
P27824	Calnexin OS=Homo sapiens OX=9606 GN=CANX PE=1 SV=2 - [CALX_HUMAN]	CALX	5	7	1.9	−1.4	−2.1	−0.4	1.1	−1.1
P28066	Proteasome subunit alpha type-5 OS=Homo sapiens OX=9606 GN=PSMA5 PE=1 SV=3 - [PSA5_HUMAN]	PSA5	2	3	−0.2	−0.9	−1.2	0.3	−0.2	−0.1
P28074	Proteasome subunit beta type-5 OS=Homo sapiens OX=9606 GN=PSMB5 PE=1 SV=3 - [PSB5_HUMAN]	PSB5	8	12	−0.9	−1.6	−0.4	2.1	−1.6	−2.1
P28838	Cytosol aminopeptidase OS=Homo sapiens OX=9606 GN=LAP3 PE=1 SV=3 - [AMPL_HUMAN]	AMPL	12	17	−0.4	−1.5	−0.5	1.0	−0.5	−1.6
P29401	Transketolase OS=Homo sapiens OX=9606 GN=TKT PE=1 SV=3 - [TKT_HUMAN]	TKT	15	17	−0.3	0.2	2.6	1.8	−1.0	−3.1
P29692	Elongation factor 1-delta OS=Homo sapiens OX=9606 GN=EEF1D PE=1 SV=5 - [EF1D_HUMAN]	EF1D	9	9	−0.2	−2.8	−0.6	−0.8	−0.8	−0.7
P30041	Peroxiredoxin-6 OS=Homo sapiens OX=9606 GN=PRDX6 PE=1 SV=3 - [PRDX6_HUMAN]	PRDX6	8	11	−0.7	−1.1	−0.1	−1.5	0.1	0.6
P30048	Thioredoxin-dependent peroxide reductase, mitochondrial OS=Homo sapiens OX=9606 GN=PRDX3 PE=1 SV=3 - [PRDX3_HUMAN]	PRDX3	3	5	−1.2	−2.0	−0.5	2.6	−1.5	−2.3
P30101	Protein disulfide-isomerase A3 OS=Homo sapiens OX=9606 GN=PDIA3 PE=1 SV=4 - [PDIA3_HUMAN]	PDIA3	9	16	0.2	−1.8	−1.3	0.8	−0.5	−1.3
P30419	Glycylpeptide N-tetradecanoyltransferase 1 OS=Homo sapiens OX=9606 GN=NMT1 PE=1 SV=2 - [NMT1_HUMAN]	NMT1	5	7	0.2	−0.5	−0.9	0.1	−1.8	−0.4
P31943	Heterogeneous nuclear ribonucleoprotein H OS=Homo sapiens OX=9606 GN=HNRNPH1 PE=1 SV=4 - [HNRH1_HUMAN]	HNRH1	15	29	−0.6	−1.5	−0.2	−0.7	−0.9	0.6
P31946	14-3-3 protein beta/alpha OS=Homo sapiens OX=9606 GN=YWHAB PE=1 SV=3 - [1433B_HUMAN]	1433B	8	14	−0.4	−0.9	−1.6	0.2	−0.4	0.0
P31948	Stress-induced-phosphoprotein 1 OS=Homo sapiens OX=9606 GN=STIP1 PE=1 SV=1 - [STIP1_HUMAN]	STIP1	4	5	0.1	−2.1	−0.9	−1.2	−0.7	0.8
P32969	60S ribosomal protein L9 OS=Homo sapiens OX=9606 GN=RPL9 PE=1 SV=1 - [RL9_HUMAN]	RL9	4	4	−0.1	0.3	1.1	1.4	−1.4	−1.7
P35232	Prohibitin OS=Homo sapiens OX=9606 GN=PHB PE=1 SV=1 - [PHB_HUMAN]	PHB	10	11	−0.5	−0.8	−0.3	−0.3	0.4	0.1
P35268	60S ribosomal protein L22 OS=Homo sapiens OX=9606 GN=RPL22 PE=1 SV=2 - [RL22_HUMAN]	RL22	2	3	−0.7	−1.7	−0.6	−2.2	1.0	2.4
P35270	Sepiapterin reductase OS=Homo sapiens OX=9606 GN=SPR PE=1 SV=1 - [SPRE_HUMAN]	SPRE	5	6	−0.2	−1.0	−1.4	−0.8	−0.9	0.0

Table 2. (continued)

P35527	Keratin, type I cytoskeletal 9 OS=Homo sapiens OX=9606 GN=KRT9 PE=1 SV=3 - [K1C9_HUMAN]	K1C9	19	28	−2.2	0.1	0.4	−0.9	−1.8	−0.9
P35579	Myosin-9 OS=Homo sapiens OX=9606 GN=MYH9 PE=1 SV=4 - [MYH9_HUMAN]	MYH9	46	58	1.2	0.6	1.1	−0.2	0.4	−0.9
P35908	Keratin, type II cytoskeletal 2 epidermal OS=Homo sapiens OX=9606 GN=KRT2 PE=1 SV=2 - [K22E_HUMAN]	K22E	27	46	−2.8	0.6	0.6	1.0	−1.8	−2.0
P36578	60S ribosomal protein L4 OS=Homo sapiens OX=9606 GN=RPL4 PE=1 SV=5 - [RL4_HUMAN]	RL4	15	16	−0.2	−1.4	−0.6	−1.3	−0.5	0.3
P36957	Dihydrolipoyllysine-residue succinyltransferase component of 2-oxoglutarate dehydrogenase complex, mitochondrial OS=Homo sapiens OX=9606 GN=DLST PE=1 SV=4 - [ODO2_HUMAN]	ODO2	5	6	0.2	−1.5	−1.1	1.5	−1.8	−0.5
P37802	Transgelin-2 OS=Homo sapiens OX=9606 GN=TAGLN2 PE=1 SV=3 - [TAGL2_HUMAN]	TAGL2	6	27	−0.9	−1.2	0.0	1.2	−1.2	−1.8
P37837	Transaldolase OS=Homo sapiens OX=9606 GN=TALDO1 PE=1 SV=2 - [TALDO_HUMAN]	TALDO	10	14	1.2	−0.9	1.2	−2.3	−1.1	−1.6
P38159	RNA-binding motif protein, X chromosome OS=Homo sapiens OX=9606 GN=RBMX PE=1 SV=3 - [RBMX_HUMAN]	RBMX	22	26	0.1	0.4	2.1	−1.5	−1.9	−1.7
P38646	Stress-70 protein, mitochondrial OS=Homo sapiens OX=9606 GN=HSPA9 PE=1 SV=2 - [GRP75_HUMAN]	GRP75	14	17	−0.2	0.1	2.7	2.2	−2.0	−0.5
P40227	T-complex protein 1 subunit zeta OS=Homo sapiens OX=9606 GN=CCT6A PE=1 SV=3 - [TCPZ_HUMAN]	TCPZ	11	15	−0.3	−1.2	−0.3	−0.4	−0.9	0.3
P40925	Malate dehydrogenase, cytoplasmic OS=Homo sapiens OX=9606 GN=MDH1 PE=1 SV=4 - [MDHC_HUMAN]	MDHC	4	5	1.1	−0.3	1.6	−1.2	−1.4	−1.8
P40926	Malate dehydrogenase, mitochondrial OS=Homo sapiens OX=9606 GN=MDH2 PE=1 SV=3 - [MDHM_HUMAN]	MDHM	17	26	1.7	−0.7	1.3	−2.3	−1.6	−1.8
P42330	Aldo-keto reductase family 1 member C3 OS=Homo sapiens OX=9606 GN=AKR1C3 PE=1 SV=4 - [AK1C3_HUMAN]	AK1C3	5	5	−0.4	−0.1	−0.4	−1.5	−0.1	0.6
P43307	Translocon-associated protein subunit alpha OS=Homo sapiens OX=9606 GN=SSR1 PE=1 SV=3 - [SSRA_HUMAN]	SSRA	2	3	−0.3	−1.2	0.2	−0.3	−0.6	−0.5
P45880	Voltage-dependent anion-selective channel protein 2 OS=Homo sapiens OX=9606 GN=VDAC2 PE=1 SV=2 - [VDAC2_HUMAN]	VDAC2	6	7	1.0	−1.3	0.0	−2.0	−1.0	−1.7
P46777	60S ribosomal protein L5 OS=Homo sapiens OX=9606 GN=RPL5 PE=1 SV=3 - [RL5_HUMAN]	RL5	11	12	0.4	−0.1	1.3	−1.0	−2.1	−1.7
P46779	60S ribosomal protein L28 OS=Homo sapiens OX=9606 GN=RPL28 PE=1 SV=3 - [RL28_HUMAN]	RL28	6	9	−0.8	−0.9	0.2	−3.0	1.9	4.2
P46782	40S ribosomal protein S5 OS=Homo sapiens OX=9606 GN=RPS5 PE=1 SV=4 - [RS5_HUMAN]	RS5	8	10	−0.9	−0.6	0.3	1.2	−1.8	−2.2
P46783	40S ribosomal protein S10 OS=Homo sapiens OX=9606 GN=RPS10 PE=1 SV=1 - [RS10_HUMAN]	RS10	7	10	−0.7	−2.0	−0.6	−2.2	1.0	2.6
P47755	F-actin-capping protein subunit alpha-2 OS=Homo sapiens OX=9606 GN=CAPZA2 PE=1 SV=3 - [CAZA2_HUMAN]	CAZA2	4	6	1.1	−1.2	0.5	−1.7	−1.1	−1.3
P48643	T-complex protein 1 subunit epsilon OS=Homo sapiens OX=9606 GN=CCT5 PE=1 SV=1 - [TCPE_HUMAN]	TCPE	5	8	0.0	−1.7	−1.0	−1.1	−0.6	0.5
P49368	T-complex protein 1 subunit gamma OS=Homo sapiens OX=9606 GN=CCT3 PE=1 SV=4 - [TCPG_HUMAN]	TCPG	13	24	0.2	−1.4	−1.0	−0.2	−1.3	0.0
P49411	Elongation factor Tu, mitochondrial OS=Homo sapiens OX=9606 GN=TUFM PE=1 SV=2 - [EFTU_HUMAN]	EFTU	7	9	1.1	−0.6	1.1	−0.9	−0.9	0.5
P49773	Histidine triad nucleotide-binding protein 1 OS=Homo sapiens OX=9606 GN=HINT1 PE=1 SV=2 - [HINT1_HUMAN]	HINT1	1	1	−1.4	−1.7	−0.5	2.3	−1.4	−1.5
P50454	Serpin H1 OS=Homo sapiens OX=9606 GN=SERPINH1 PE=1 SV=2 - [SERPH_HUMAN]	SERPH	11	15	0.1	−1.9	−1.3	−1.1	−0.8	0.5
P50990	T-complex protein 1 subunit theta OS=Homo sapiens OX=9606 GN=CCT8 PE=1 SV=4 - [TCPQ_HUMAN]	TCPQ	10	13	−0.3	−1.4	−0.7	−1.1	−0.4	0.7
P50991	T-complex protein 1 subunit delta OS=Homo sapiens OX=9606 GN=CCT4 PE=1 SV=4 - [TCPD_HUMAN]	TCPD	15	18	−0.7	−1.3	−0.7	1.1	−0.7	−2.1
P50993	Sodium/potassium-transporting ATPase subunit alpha-2 OS=Homo sapiens OX=9606 GN=ATP1A2 PE=1 SV=1 - [AT1A2_HUMAN]	AT1A2	15	24	0.3	−1.2	−0.8	1.3	−2.6	−1.1
P51148	Ras-related protein Rab-5C OS=Homo sapiens OX=9606 GN=RAB5C PE=1 SV=2 - [RAB5C_HUMAN]	RAB5C	7	10	−0.2	−3.4	0.2	1.3	−2.9	−1.8
P51149	Ras-related protein Rab-7a OS=Homo sapiens OX=9606 GN=RAB7A PE=1 SV=1 - [RAB7A_HUMAN]	RAB7A	4	7	−0.5	−2.0	−0.7	1.1	−1.0	−0.8
P51665	26S proteasome non-ATPase regulatory subunit 7 OS=Homo sapiens OX=9606 GN=PSMD7 PE=1 SV=2 - [PSMD7_HUMAN]	PSMD7	3	6	−0.2	−1.6	−1.3	−1.8	−1.6	−3.0
P52272	Heterogeneous nuclear ribonucleoprotein M OS=Homo sapiens OX=9606 GN=HNRNPM PE=1 SV=3 - [HNRPM_HUMAN]	HNRPM	39	61	−0.7	0.2	1.9	1.7	−1.9	−0.4
P52758	2-iminobutanoate/2-iminopropanoate deaminase OS=Homo sapiens OX=9606 GN=RIDA PE=1 SV=1 - [RIDA_HUMAN]	RIDA	3	5	−0.2	−1.1	0.6	1.9	−1.2	−1.5
P52895	Aldo-keto reductase family 1 member C2 OS=Homo sapiens OX=9606 GN=AKR1C2 PE=1 SV=3 - [AK1C2_HUMAN]	AK1C2	6	9	0.0	−1.1	−0.9	0.5	−1.2	0.0
P52907	F-actin-capping protein subunit alpha-1 OS=Homo sapiens OX=9606 GN=CAPZA1 PE=1 SV=3 - [CAZA1_HUMAN]	CAZA1	4	6	0.0	−1.5	−1.1	0.0	−1.6	−1.1
P53396	ATP-citrate synthase OS=Homo sapiens OX=9606 GN=ACLY PE=1 SV=3 - [ACLY_HUMAN]	ACLY	15	21	2.0	−1.2	−2.2	−0.9	−0.1	0.4
P55072	Transitional endoplasmic reticulum ATPase OS=Homo sapiens OX=9606 GN=VCP PE=1 SV=4 - [TERA_HUMAN]	TERA	21	29	0.5	−1.3	−1.1	−0.2	0.5	−0.7
P55209	Nucleosome assembly protein 1-like 1 OS=Homo sapiens OX=9606 GN=NAP1L1 PE=1 SV=1 - [NP1L1_HUMAN]	NP1L1	4	6	0.1	−2.0	−1.3	−2.2	0.5	1.7
P57735	Ras-related protein Rab-25 OS=Homo sapiens OX=9606 GN=RAB25 PE=1 SV=2 - [RAB25_HUMAN]	RAB25	7	17	0.4	0.3	0.6	1.0	−1.2	−1.1

Table 2. (continued)

P60174	Triosephosphate isomerase OS=Homo sapiens OX=9606 GN=TPI1 PE=1 SV=3 - [TPIS_HUMAN]	TPIS	10	14	−0.8	−1.7	−0.6	3.1	−1.8	−2.4
P60709	Actin, cytoplasmic 1 OS=Homo sapiens OX=9606 GN=ACTB PE=1 SV=1 - [ACTB_HUMAN]	ACTB	32	153	1.4	−1.3	0.8	−2.3	−0.9	−0.7
P60842	Eukaryotic initiation factor 4A-I OS=Homo sapiens OX=9606 GN=EIF4A1 PE=1 SV=1 - [IF4A1_HUMAN]	IF4A1	14	22	−0.6	−1.1	−0.6	−1.2	−0.6	0.9
P60866	40S ribosomal protein S20 OS=Homo sapiens OX=9606 GN=RPS20 PE=1 SV=1 - [RS20_HUMAN]	RS20	4	5	−1.4	−0.8	0.5	1.2	−1.0	−0.8
P61160	Actin-related protein 2 OS=Homo sapiens OX=9606 GN=ACTR2 PE=1 SV=1 - [ARP2_HUMAN]	ARP2	7	7	0.2	−2.3	−1.7	−1.1	−0.5	0.5
P61247	40S ribosomal protein S3a OS=Homo sapiens OX=9606 GN=RPS3A PE=1 SV=2 - [RS3A_HUMAN]	RS3A	16	22	1.6	−0.5	2.2	−1.3	−2.2	−1.9
P61353	60S ribosomal protein L27 OS=Homo sapiens OX=9606 GN=RPL27 PE=1 SV=2 - [RL27_HUMAN]	RL27	5	5	−0.6	−2.3	−0.9	−4.3	2.7	3.8
P61604	10 kDa heat shock protein, mitochondrial OS=Homo sapiens OX=9606 GN=HSPE1 PE=1 SV=2 - [CH10_HUMAN]	CH10	7	13	−1.1	−1.3	0.5	1.6	−1.0	−0.9
P61978	Heterogeneous nuclear ribonucleoprotein K OS=Homo sapiens OX=9606 GN=HNRNPK PE=1 SV=1 - [HNRPK_HUMAN]	HNRPK	17	28	0.2	−2.1	−1.5	−0.5	−1.0	0.4
P61981	14-3-3 protein gamma OS=Homo sapiens OX=9606 GN=YWHAG PE=1 SV=2 - [1433G_HUMAN]	1433G	6	7	−0.3	−1.2	−1.4	−1.1	0.9	0.7
P62081	40S ribosomal protein S7 OS=Homo sapiens OX=9606 GN=RPS7 PE=1 SV=1 - [RS7_HUMAN]	RS7	8	13	−1.4	−1.3	0.1	2.0	−1.3	−1.7
P62244	40S ribosomal protein S15a OS=Homo sapiens OX=9606 GN=RPS15A PE=1 SV=2 - [RS15A_HUMAN]	RS15A	4	4	−0.4	−2.8	−1.2	−3.2	1.7	2.7
P62249	40S ribosomal protein S16 OS=Homo sapiens OX=9606 GN=RPS16 PE=1 SV=2 - [RS16_HUMAN]	RS16	7	12	−0.7	−1.0	0.0	0.9	−1.1	−0.3
P62258	14-3-3 protein epsilon OS=Homo sapiens OX=9606 GN=YWHAE PE=1 SV=1 - [1433E_HUMAN]	1433E	9	16	0.0	−0.8	−1.0	−1.4	−1.4	−1.5
P62266	40S ribosomal protein S23 OS=Homo sapiens OX=9606 GN=RPS23 PE=1 SV=3 - [RS23_HUMAN]	RS23	5	9	−0.8	−1.0	0.4	1.2	−1.4	−1.9
P62269	40S ribosomal protein S18 OS=Homo sapiens OX=9606 GN=RPS18 PE=1 SV=3 - [RS18_HUMAN]	RS18	4	6	−0.6	−1.3	−0.4	−2.7	1.2	2.9
P62277	40S ribosomal protein S13 OS=Homo sapiens OX=9606 GN=RPS13 PE=1 SV=2 - [RS13_HUMAN]	RS13	8	10	−1.0	−1.0	0.6	−3.0	1.1	3.1
P62424	60S ribosomal protein L7a OS=Homo sapiens OX=9606 GN=RPL7A PE=1 SV=2 - [RL7A_HUMAN]	RL7A	6	6	−0.4	−1.8	−0.8	0.6	−0.1	0.0
P62701	40S ribosomal protein S4, X isoform OS=Homo sapiens OX=9606 GN=RPS4X PE=1 SV=2 - [RS4X_HUMAN]	RS4X	4	4	−0.1	−1.1	−1.1	2.4	−1.9	−3.1
P62805	Histone H4 OS=Homo sapiens OX=9606 GN=HIST1H4A PE=1 SV=2 - [H4_HUMAN]	H4	11	47	−1.6	−1.0	0.5	2.8	−3.1	−3.8
P62826	GTP-binding nuclear protein Ran OS=Homo sapiens OX=9606 GN=RAN PE=1 SV=3 - [RAN_HUMAN]	RAN	8	12	−1.4	−1.5	−0.2	2.9	−2.0	−2.5
P62851	40S ribosomal protein S25 OS=Homo sapiens OX=9606 GN=RPS25 PE=1 SV=1 - [RS25_HUMAN]	RS25	4	6	−1.6	−1.0	0.7	2.9	−2.1	−2.2
P62857	40S ribosomal protein S28 OS=Homo sapiens OX=9606 GN=RPS28 PE=1 SV=1 - [RS28_HUMAN]	RS28	5	14	−2.8	−1.5	0.3	−3.1	2.0	3.9
P62899	60S ribosomal protein L31 OS=Homo sapiens OX=9606 GN=RPL31 PE=1 SV=1 - [RL31_HUMAN]	RL31	3	4	−0.8	−1.5	−0.4	−2.8	1.1	2.5
P62910	60S ribosomal protein L32 OS=Homo sapiens OX=9606 GN=RPL32 PE=1 SV=2 - [RL32_HUMAN]	RL32	4	5	−0.9	−0.9	0.9	1.3	−1.1	−1.8
P62917	60S ribosomal protein L8 OS=Homo sapiens OX=9606 GN=RPL8 PE=1 SV=2 - [RL8_HUMAN]	RL8	12	13	1.0	−0.5	1.6	−1.1	−1.5	−1.8
P62937	Peptidyl-prolyl cis-trans isomerase A OS=Homo sapiens OX=9606 GN=PPIA PE=1 SV=2 - [PPIA_HUMAN]	PPIA	10	22	−1.4	−1.3	0.4	1.9	−1.5	−2.7
P62979	Ubiquitin-40S ribosomal protein S27a OS=Homo sapiens OX=9606 GN=RPS27A PE=1 SV=2 - [RS27A_HUMAN]	RS27A	8	19	−1.5	−1.7	0.5	2.2	−2.3	−2.7
P62995	Transformer-2 protein homolog beta OS=Homo sapiens OX=9606 GN=TRA2B PE=1 SV=1 - [TRA2B_HUMAN]	TRA2B	11	16	0.9	−1.1	0.9	0.2	−1.9	−0.8
P63104	14-3-3 protein zeta/delta OS=Homo sapiens OX=9606 GN=YWHAZ PE=1 SV=1 - [1433Z_HUMAN]	1433Z	14	36	−0.9	−1.7	−0.3	−0.4	0.2	0.3
P63244	Receptor of activated protein C kinase 1 OS=Homo sapiens OX=9606 GN=RACK1 PE=1 SV=3 - [RACK1_HUMAN]	RACK1	13	19	−1.1	−1.2	−0.4	−2.2	−2.2	−1.3
P68104	Elongation factor 1-alpha 1 OS=Homo sapiens OX=9606 GN=EEF1A1 PE=1 SV=1 - [EF1A1_HUMAN]	EF1A1	16	31	−0.9	−1.7	−1.0	1.3	−0.9	−2.5
P68133	Actin, alpha skeletal muscle OS=Homo sapiens OX=9606 GN=ACTA1 PE=1 SV=1 - [ACTS_HUMAN]	ACTS	16	61	0.9	−1.7	−2.3	−2.4	−2.1	−1.4
P68371	Tubulin beta-4B chain OS=Homo sapiens OX=9606 GN=TUBB4B PE=1 SV=1 - [TBB4B_HUMAN]	TBB4B	20	44	−0.3	−1.3	−0.4	0.9	−0.6	−1.2
P68431	Histone H3.1 OS=Homo sapiens OX=9606 GN=HIST1H3A PE=1 SV=2 - [H31_HUMAN]	H31	8	13	0.2	1.2	1.7	2.5	−1.9	−2.4
P78371	T-complex protein 1 subunit beta OS=Homo sapiens OX=9606 GN=CCT2 PE=1 SV=4 - [TCPB_HUMAN]	TCPB	17	19	−0.5	−1.6	−0.9	1.8	−0.3	−2.4
P81605	Dermcidin OS=Homo sapiens OX=9606 GN=DCD PE=1 SV=2 - [DCD_HUMAN]	DCD	4	5	−1.4	0.3	0.7	1.6	−2.4	−2.7
Q00534	Cyclin-dependent kinase 6 OS=Homo sapiens OX=9606 GN=CDK6 PE=1 SV=1 - [CDK6_HUMAN]	CDK6	8	11	−0.1	−0.9	−1.1	−1.1	−1.0	−1.3
Q00610	Clathrin heavy chain 1 OS=Homo sapiens OX=9606 GN=CLTC PE=1 SV=5 - [CLH1_HUMAN]	CLH1	26	29	0.3	−1.4	−1.2	−2.1	1.0	2.8
Q00839	Heterogeneous nuclear ribonucleoprotein U OS=Homo sapiens OX=9606 GN=HNRNPU PE=1 SV=6 - [HNRPU_HUMAN]	HNRPU	14	15	0.0	−1.0	−0.7	1.3	−2.8	−1.0
Q02878	60S ribosomal protein L6 OS=Homo sapiens OX=9606 GN=RPL6 PE=1 SV=3 - [RL6_HUMAN]	RL6	5	7	−0.2	−0.9	−1.9	−3.5	2.0	1.3
Q03252	Lamin-B2 OS=Homo sapiens OX=9606 GN=LMNB2 PE=1 SV=4 - [LMNB2_HUMAN]	LMNB2	21	26	−0.2	−1.7	−0.8	2.1	−0.5	−2.6

Table 2. (continued)

Q04828	Aldo-keto reductase family 1 member C1 OS=Homo sapiens OX=9606 GN=AKR1C1 PE=1 SV=1 - [AK1C1_HUMAN]	AK1C1	5	7	−0.1	−1.1	−0.8	−1.3	−1.2	−1.0
Q04917	14-3-3 protein eta OS=Homo sapiens OX=9606 GN=YWHAH PE=1 SV=4 - [1433F_HUMAN]	1433F	6	6	−1.5	−0.3	−1.7	−0.7	−0.6	0.2
Q06830	Peroxiredoxin-1 OS=Homo sapiens OX=9606 GN=PRDX1 PE=1 SV=1 - [PRDX1_HUMAN]	PRDX1	12	30	−1.3	−1.3	−0.2	1.4	−1.7	−1.9
Q07065	Cytoskeleton-associated protein 4 OS=Homo sapiens OX=9606 GN=CKAP4 PE=1 SV=2 - [CKAP4_HUMAN]	CKAP4	5	6	0.1	−2.4	−1.1	−1.7	0.3	1.4
Q07955	Serine/arginine-rich splicing factor 1 OS=Homo sapiens OX=9606 GN=SRSF1 PE=1 SV=2 - [SRSF1_HUMAN]	SRSF1	15	22	−0.7	−1.6	−0.7	−1.5	−1.0	−1.4
Q08257	Quinone oxidoreductase OS=Homo sapiens OX=9606 GN=CRYZ PE=1 SV=1 - [QOR_HUMAN]	QOR	7	13	−0.3	−1.1	−1.8	−1.4	−1.0	−1.0
Q13162	Peroxiredoxin-4 OS=Homo sapiens OX=9606 GN=PRDX4 PE=1 SV=1 - [PRDX4_HUMAN]	PRDX4	5	12	−0.8	−0.6	−0.6	1.2	−1.2	−1.4
Q13442	28 kDa heat- and acid-stable phosphoprotein OS=Homo sapiens OX=9606 GN=PDAP1 PE=1 SV=1 - [HAP28_HUMAN]	HAP28	4	4	−0.5	0.2	0.6	0.7	−1.1	−0.7
Q14315	Filamin-C OS=Homo sapiens OX=9606 GN=FLNC PE=1 SV=3 - [FLNC_HUMAN]	FLNC	34	45	−1.5	0.1	0.6	1.6	−2.8	−1.3
Q14376	UDP-glucose 4-epimerase OS=Homo sapiens OX=9606 GN=GALE PE=1 SV=2 - [GALE_HUMAN]	GALE	2	2	0.0	−1.6	−1.0	0.0	−0.9	−0.1
Q14847	LIM and SH3 domain protein 1 OS=Homo sapiens OX=9606 GN=LASP1 PE=1 SV=2 - [LASP1_HUMAN]	LASP1	8	8	0.2	−1.6	−1.5	1.3	−0.4	−1.6
Q14974	Importin subunit beta-1 OS=Homo sapiens OX=9606 GN=KPNB1 PE=1 SV=2 - [IMB1_HUMAN]	IMB1	10	13	−1.4	−0.5	0.4	−0.1	0.3	−0.2
Q15008	26S proteasome non-ATPase regulatory subunit 6 OS=Homo sapiens OX=9606 GN=PSMD6 PE=1 SV=1 - [PSMD6_HUMAN]	PSMD6	8	15	−0.1	−1.6	−0.7	−0.7	−1.5	−1.4
Q15084	Protein disulfide-isomerase A6 OS=Homo sapiens OX=9606 GN=PDIA6 PE=1 SV=1 - [PDIA6_HUMAN]	PDIA6	10	16	−0.4	−0.1	1.5	−2.4	0.5	1.2
Q15181	Inorganic pyrophosphatase OS=Homo sapiens OX=9606 GN=PPA1 PE=1 SV=2 - [IPYR_HUMAN]	IPYR	5	8	1.2	−0.8	1.3	−1.2	−2.0	−2.3
Q15233	Non-POU domain-containing octamer-binding protein OS=Homo sapiens OX=9606 GN=NONO PE=1 SV=4 - [NONO_HUMAN]	NONO	11	14	0.0	−0.3	2.6	−0.8	−1.0	0.2
Q15366	Poly(rC)-binding protein 2 OS=Homo sapiens OX=9606 GN=PCBP2 PE=1 SV=1 - [PCBP2_HUMAN]	PCBP2	7	9	−0.5	−1.4	−1.3	−2.7	−1.3	−1.2
Q15417	Calponin-3 OS=Homo sapiens OX=9606 GN=CNN3 PE=1 SV=1 - [CNN3_HUMAN]	CNN3	9	11	0.7	−0.5	1.2	−1.4	−1.2	−1.3
Q5VTE0	Putative elongation factor 1-alpha-like 3 OS=Homo sapiens OX=9606 GN=EEF1A1P5 PE=5 SV=1 - [EF1A3_HUMAN]	EF1A3	14	26	0.1	−2.6	−0.8	−1.9	−0.3	1.1
Q6PI78	Transmembrane protein 65 OS=Homo sapiens OX=9606 GN=TMEM65 PE=1 SV=2 - [TMM65_HUMAN]	TMM65	1	1	0.2	−1.6	−1.2	−0.3	−1.1	0.2
Q6ZRQ5	Protein MMS22-like OS=Homo sapiens OX=9606 GN=MMS22L PE=1 SV=3 - [MMS22_HUMAN]	MMS22	15	25	1.2	−0.3	3.1	−0.1	0.1	0.0
Q86XK2	F-box only protein 11 OS=Homo sapiens OX=9606 GN=FBXO11 PE=1 SV=3 - [FBX11_HUMAN]	FBX11	8	13	0.9	−3.0	−0.6	−0.1	0.1	0.0
Q8IYB7	DIS3-like exonuclease 2 OS=Homo sapiens OX=9606 GN=DIS3L2 PE=1 SV=4 - [DI3L2_HUMAN]	DI3L2	7	9	−0.6	−1.2	−0.3	0.3	−3.9	0.7
Q8N257	Histone H2B type 3-B OS=Homo sapiens OX=9606 GN=HIST3H2BB PE=1 SV=3 - [H2B3B_HUMAN]	H2B3B	10	49	−1.2	−0.8	0.4	1.0	−1.0	−1.7
Q8NBS9	Thioredoxin domain-containing protein 5 OS=Homo sapiens OX=9606 GN=TXNDC5 PE=1 SV=2 - [TXND5_HUMAN]	TXND5	5	7	0.1	−1.5	−1.1	−0.9	−1.0	0.4
Q969Z0	FAST kinase domain-containing protein 4 OS=Homo sapiens OX=9606 GN=TBRG4 PE=1 SV=1 - [FAKD4_HUMAN]	FAKD4	10	13	0.0	0.2	1.8	−0.1	−0.2	−0.2
Q96C19	EF-hand domain-containing protein D2 OS=Homo sapiens OX=9606 GN=EFHD2 PE=1 SV=1 - [EFHD2_HUMAN]	EFHD2	7	8	−0.1	−1.0	−1.1	−1.5	−0.9	−0.8
Q99497	Protein/nucleic acid deglycase DJ-1 OS=Homo sapiens OX=9606 GN=PARK7 PE=1 SV=2 - [PARK7_HUMAN]	PARK7	4	14	−0.6	−0.9	−0.1	2.1	−1.4	−1.6
Q99623	Prohibitin-2 OS=Homo sapiens OX=9606 GN=PHB2 PE=1 SV=2 - [PHB2_HUMAN]	PHB2	11	16	−0.4	−2.0	−0.5	−1.7	−1.3	−1.2
Q99714	3-hydroxyacyl-CoA dehydrogenase type-2 OS=Homo sapiens OX=9606 GN=HSD17B10 PE=1 SV=3 - [HCD2_HUMAN]	HCD2	5	7	−0.3	−1.3	−0.8	0.8	−1.0	−0.9
Q99729	Heterogeneous nuclear ribonucleoprotein A/B OS=Homo sapiens OX=9606 GN=HNRNPAB PE=1 SV=2 - [ROAA_HUMAN]	ROAA	4	4	0.2	−1.9	−0.9	0.0	−1.3	0.2
Q99832	T-complex protein 1 subunit eta OS=Homo sapiens OX=9606 GN=CCT7 PE=1 SV=2 - [TCPH_HUMAN]	TCPH	11	15	0.1	−1.3	−0.6	−0.6	−1.0	0.2
Q9BPU6	Dihydropyrimidinase-related protein 5 OS=Homo sapiens OX=9606 GN=DPYSL5 PE=1 SV=1 - [DPYL5_HUMAN]	DPYL5	3	6	−0.8	−0.9	0.4	1.4	−1.2	−1.8
Q9BQE3	Tubulin alpha-1C chain OS=Homo sapiens OX=9606 GN=TUBA1C PE=1 SV=1 - [TBA1C_HUMAN]	TBA1C	21	41	−0.5	−1.5	−0.5	−0.6	−1.2	0.4
Q9BTM1	Histone H2A.J OS=Homo sapiens OX=9606 GN=H2AFJ PE=1 SV=1 - [H2AJ_HUMAN]	H2AJ	6	16	−1.4	−1.2	−0.2	1.1	−1.1	−1.7
Q9H0C2	ADP/ATP translocase 4 OS=Homo sapiens OX=9606 GN=SLC25A31 PE=2 SV=1 - [ADT4_HUMAN]	ADT4	10	12	0.2	0.3	1.6	−0.7	1.0	−0.5
Q9H0E2	Toll-interacting protein OS=Homo sapiens OX=9606 GN=TOLLIP PE=1 SV=1 - [TOLIP_HUMAN]	TOLIP	3	3	−0.2	−0.4	1.2	0.6	−0.7	−0.2
Q9NR45	Sialic acid synthase OS=Homo sapiens OX=9606 GN=NANS PE=1 SV=2 - [SIAS_HUMAN]	SIAS	8	10	1.0	0.1	1.6	−1.5	−0.9	−0.9
Q9NRX3	NADH dehydrogenase [ubiquinone] 1 alpha subcomplex subunit 4-like 2 OS=Homo sapiens OX=9606 GN=NDUFA4L2 PE=3 SV=1 - [NUA4L_HUMAN]	NDUFA4L2	2	2	−0.1	0.1	0.0	0.4	−1.7	−0.9
Q9NSD9	Phenylalanine--tRNA ligase beta subunit OS=Homo sapiens OX=9606 GN=FARSB PE=1 SV=3 - [SYFB_HUMAN]	SYFB	4	4	0.3	−1.4	−1.1	0.2	−1.7	−0.2

Table 2. (continued)

Q9P219	Protein Daple OS=Homo sapiens OX=9606 GN=CCDC88C PE=1 SV=3 - [DAPLE_HUMAN]	DAPLE	36	47	−0.1	0.8	0.8	0.1	−1.5	−0.2
Q9UBQ5	Eukaryotic translation initiation factor 3 subunit K OS=Homo sapiens OX=9606 GN=EIF3K PE=1 SV=1 - [EIF3K_HUMAN]	EIF3K	3	7	−0.7	−0.8	−0.2	0.1	−1.4	0.6
Q9UHV9	Prefoldin subunit 2 OS=Homo sapiens OX=9606 GN=PFDN2 PE=1 SV=1 - [PFD2_HUMAN]	PFD2	3	4	0.2	−0.3	0.3	0.5	−0.8	−0.4
Q9UL46	Proteasome activator complex subunit 2 OS=Homo sapiens OX=9606 GN=PSME2 PE=1 SV=4 - [PSME2_HUMAN]	PSME2	7	14	1.0	−0.9	0.9	−1.4	−1.3	−1.1
Q9ULE4	Protein FAM184B OS=Homo sapiens OX=9606 GN=FAM184B PE=2 SV=3 - [F184B_HUMAN]	F184B	18	20	1.9	−0.8	1.2	−1.9	−2.0	−2.0
Q9UMS4	Pre-mRNA-processing factor 19 OS=Homo sapiens OX=9606 GN=PRPF19 PE=1 SV=1 - [PRP19_HUMAN]	PRP19	2	3	0.2	−1.3	−1.2	−0.3	−1.5	−0.1
Q9UNM6	26S proteasome non-ATPase regulatory subunit 13 OS=Homo sapiens OX=9606 GN=PSMD13 PE=1 SV=2 - [PSD13_HUMAN]	PSD13	1	1	−0.2	−1.2	−0.9	−1.8	−1.5	−2.3
Q9UQ05	Potassium voltage-gated channel subfamily H member 4 OS=Homo sapiens OX=9606 GN=KCNH4 PE=2 SV=1 - [KCNH4_HUMAN]	KCNH4	11	13	−0.2	−4.0	−6.6	0.9	−2.6	−0.9
Q9Y230	RuvB-like 2 OS=Homo sapiens OX=9606 GN=RUVBL2 PE=1 SV=3 - [RUVB2_HUMAN]	RUVB2	6	8	0.2	−1.6	−1.3	−0.5	−1.1	0.2
Q9Y265	RuvB-like 1 OS=Homo sapiens OX=9606 GN=RUVBL1 PE=1 SV=1 - [RUVB1_HUMAN]	RUVB1	3	5	0.2	−1.4	−1.2	2.7	−3.3	−0.3
Q9Y617	Phosphoserine aminotransferase OS=Homo sapiens OX=9606 GN=PSAT1 PE=1 SV=2 - [SERC_HUMAN]	SERC	1	2	−0.6	−1.2	−0.9	−2.0	−1.5	−1.1
Q2TB90	Putative hexokinase HKDC1 OS=Homo sapiens OX=9606 GN=HKDC1 PE=1 SV=3 - [HKDC1_HUMAN]	HKDC1	14	18	1.0	0.1	1.5	1.7	−3.1	−1.3
Q86YZ3	Hornerin OS=Homo sapiens OX=9606 GN=HRNR PE=1 SV=2 - [HORN_HUMAN]	HORN	21	31	−1.5	−0.2	−1.1	1.4	−1.9	−1.8

Table 2. List of proteins expressed in the vero cells post infection, infection and gramicidin S treatment and infection and melittin treatment for 24 and 48 h post infection.

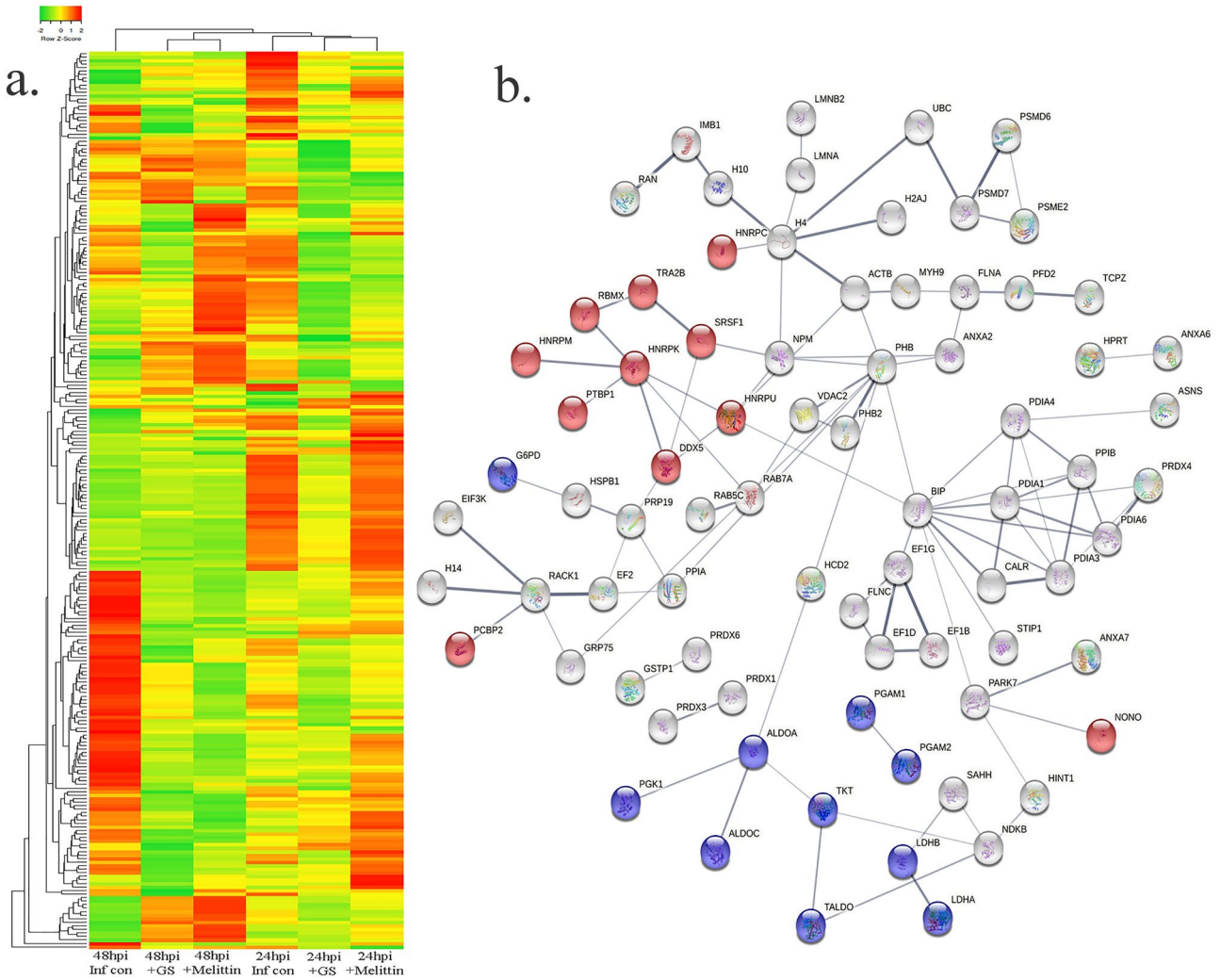

Figure 5. (**a**) Heat map expression of proteins in Vero cells post infection and peptide treatment. The image was created using web-enabled heatmapper software. (**b**) Network pathway analysis of the differentially expressed protein based on STRING analysis. The image was created using web-enabled STRING v11 software.

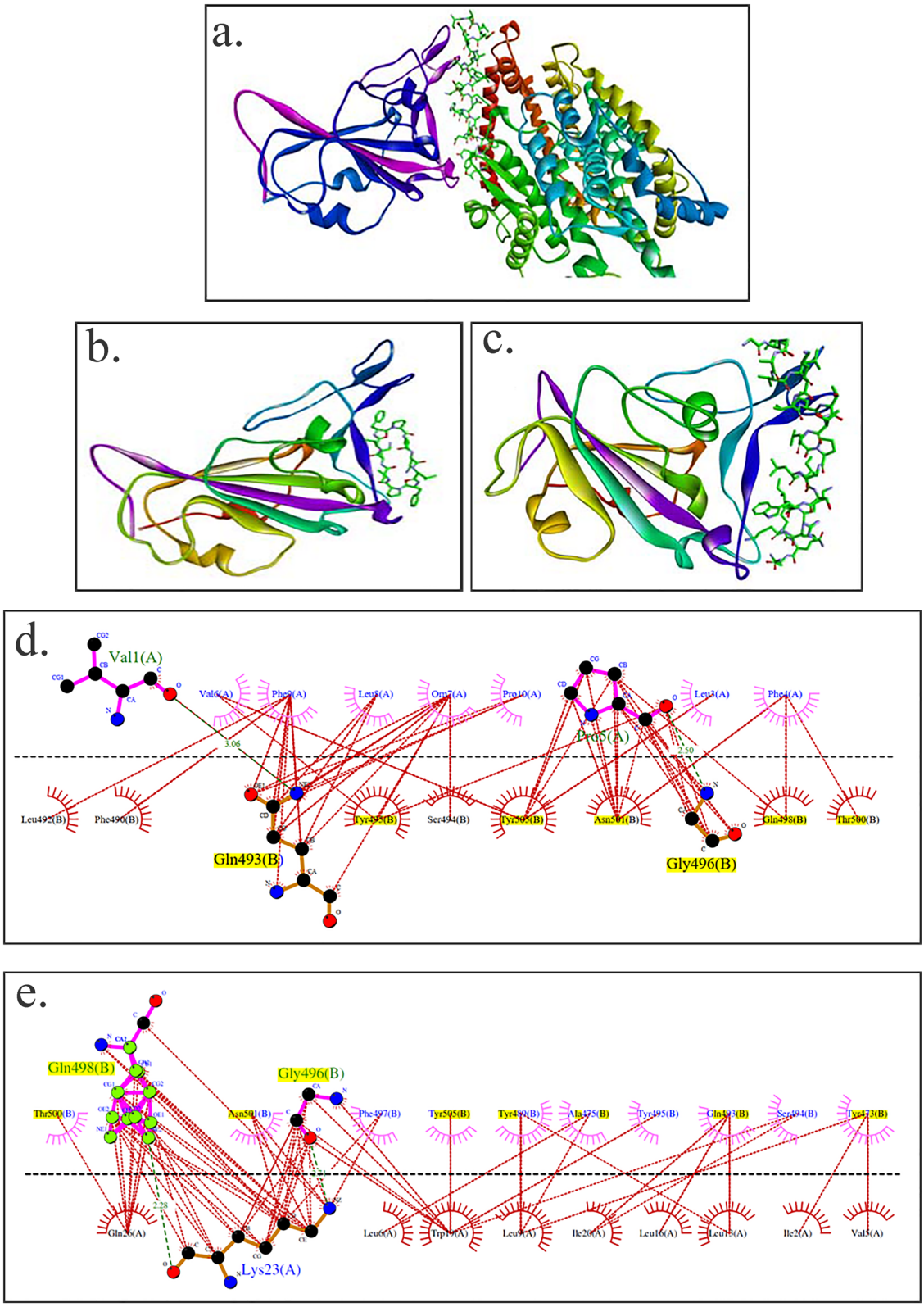

Figure 6. Structures of RBD of spike proteins and peptides and RBD binding region of ACE 2. (**a**) RBD and ACE, (**b**) RBD and gramicidin S, (**c**) RBD and melittin. The ACE2 binding region in RBD is colored violet. In ACE2, gramicidin S and melittin, the peptide regions binding to RBD are represented as sticks. LigPlots of interaction between ACE2 binding domain of the spike protein and (**d**) gramicidin S and (**e**) melittin. The residues of the RBD involved in binding to ACE2 are in yellow. The structures in panel (**a**–**c**) were generated using Discovery Studio v19.1.0.18287. The figures in panel (**d**, **e**) were generated using LigPlot.

other viral infections. In case of HIV, drugs specific to the virus has been effective to treat the disease although there is still no effective vaccine. Likewise, malaria can be treated with specific drugs rather than vaccines.

However, development of specific therapeutic antiviral drugs for clinical use in a short span is extremely challenging. Repurposing of drugs already known for their therapeutic effects have been extensively screened and tested for inhibition of SARS-CoV-2[1,6]. While many repurposed drugs have shown excellent anti SARS-CoV-2 activity in vitro, they have shown very little success when used clinically. We have shown that host defence peptide such as β-defensins may have a role in infection by SARS-CoV-2 as they are down regulated in COVID-19 patients[31].

Bee venom has immunosuppressive activity and is generally used in contemporary medicine to treat Multiple Sclerosis, Parkinson's disease, and arthritis. Bee venom activates foxP3-expressing cells, CD25 and CD4 + T cells, and thus modulates the IgE antibody ratio, resulting in a variety of allergic reactions to antigens[32]. This immunosuppressive activity was observed in Wuhan beekeepers against COVID-19[32]. Melittin is the main component of bee venom, and it is active against both enveloped and non-enveloped viruses by activating the Toll-like receptors (TLRs) pathway, which reduces inflammatory cytokines like nuclear factor-kappa B (NF-kB), extracellular signal-regulated kinases (ERK1/2), and protein kinase Akt[32]. Melittin exhibited antiviral activity against several viruses in vitro[18]. Significant antiviral activity of the sitagliptin and melittin-nanoconjugates complex (IC50 value-8.439 μM) was observed against SARS-CoV-2 in vitro[19]. Binding of sitagliptin and melittin nano conjugates to the active site of SARS-CoV-2 3CLpro (a protease) was also observed through molecular docking[19].

Gramicidin S has potent antibacterial and fungicidal activity[13]. Molecular docking revealed that gramicidin S has a binding affinity of 11.4 kcal/mol to the SARS-CoV-2 spike glycoprotein and SARS-CoV-2 papain like protease, implying that gramicidin S could be an effective drug against the SARS-CoV-2 virus[33]. SARS-CoV-2 is an enveloped virus, with the viral membrane essential for its integrity and function[1,10]. We reasoned that membrane-active peptides would disrupt the viral membrane and render the virus ineffective. We have investigated the anti-SARS-CoV-2 activity of two well studied membrane-active antibacterial peptides gramicidin S and melittin.

Our present in vitro studies using gramicidin S and melittin showed EC_{50} value of 1.571 μg for gramicidin S and 0.656 μg for melittin (Fig. 1). The results were comparable with remdesivir which we used as the assay control in our study (Fig. 5). The immunofluorescence studies are in agreement with our RT-qPCR data showing the decrease in the viral load in the gramicidin S and melittin treated experimental groups compared to peptide non treated group (Fig. 4). Molecular docking studies suggest that both the peptides have structural features that would favor binding to RBD of the spike protein (Fig. 6). ZDOCK used in the present study, has been used extensively to study protein–protein/peptide interactions[34]. However, our prediction that melittin and gramicidin S have structural features that favor interaction with RBD needs experimental validation. In fact, membrane-active antibacterial peptides have multiple targets in bacteria. It is conceivable that gramicidin S and melittin also have multiple targets on the virus thereby acting as an effective antiviral agent. Both gramicidin S and melittin have hemolytic activity at concentrations higher than the EC50 values reported in this study. Hemolytic activity can be attenuated or eliminated by engineering the peptide for specific antiviral activity. This approach has been successfully used in generating gramicidin S and melittin analogs with only antibacterial activity without any hemolytic activity[35,36]. In order to prevent off-target toxic effects of melittin, formulations with polymeric nanoparticles are being explored[37]. Formulations for use of peptides as therapeutics is a challenge but there are considerable efforts towards this goal[12].

Proteomics studies indicate that metabolic change caused by SARS-CoV-2 pathogenesis result in long-term metabolic disorders in COVID-19 patients, and this varies according to pathogen severity. Carbon sources, specifically glycolysis and glutamino lysis pathways, have been found to play critical roles in SARS-CoV-2 viral replication and production[38]. Non-oxidative pentose phosphate pathways (PPP) are also involved in viral replication; Transketolase is a key mediator enzyme of PPP involved in ribonucleotide production. Benfo-oxythiamine, a TKT inhibitor, acted against SARS-CoV-2 infection and inhibited the viral replication[39]. Our findings from proteomic pathway analysis showed that several proteins are strongly associated with carbon metabolism and non-oxidative PPP. Specifically, LDHA, LDHB, ALDOA, TALDO, PGK1, and PGAM2 proteins were found to be up regulated in early viral replication, i.e. at 24 h viral induced cell control, and vice versa in gramicidin-treated cells. TKT was found to be up regulated after 48 h of viral induced cell control, but it was substantially down regulated by melittin treatment. It suggests that gramicidin and melittin may function as viral inhibitors by suppressing intercellular metabolic regulators.

Another prominent pathway, mRNA processing, was identified during the local network pathway analysis. According to a recent study on SARS-CoV-2 RNA host protein interaction, the majority of virus which induced host RNA binding proteins prevents the virus induced cell death. Several mRNA binding proteins, including Heterogeneous nuclear ribonucleoproteins (HNRNPs), dead box RNA helicases (DDX), and NONO, were activated during the innate immune response to SARS-CoV-2 infection[40]. In our study, NONO, DDX5, RBMX, and HNRPM proteins were found to be up regulated with more than 1 log fold change in melittin-treated SARS-CoV-2 infected cells. This finding suggests that melittin may have antiviral activity during the early stages of viral infection by activating host RNA binding proteins.

The antimicrobial activity of gramicidin S and melittin have been well characterized. Our results strongly argue for development of peptides, gramicidin S and melittin, as potent therapeutic candidates to treat SARS-CoV-2 and possibly other influenza like viruses which are also enveloped viruses, for which there are no effective vaccines. Localized delivery at the site of infection in the nasopharyngeal region by appropriate formulations would avoid cytotoxicity due to systemic delivery.

In conclusion, our study indicates the potential of antibacterial peptides such as gramicidin S and melittin for development as therapeutic molecules to treat COVID19. These peptides have broad-spectrum antibacterial activity and resistance does not develop against them. It is likely that variants of SARS-CoV-2 which may escape immune surveillance, may be susceptible to membrane-active peptides such as gramicidin S and melittin.

With tremendous advances in the formulation of drugs to minimize side-effects, it should be able to administer gramicidin S and melittin by appropriate formulations to avoid any non-specific cytolytic effects.

Materials and methods

Peptides. Gramicidin S and melittin were procured from commercial sources (Gramicidin S: 368108, Calbiochem CA, USA Melittin: M4171 from Sigma Chemical Co, USA). They were characterized by HPLC and mass spectrometry and found to be > 95% pure.

Cell viability using MTT assay. The Vero cells were plated in 96 well culture plate and incubated at 37 °C with 5% CO_2. After attaining 90–95% cell confluency, different concentrations of gramicidin S and melittin (0.5, 0.7, 3, 5 µg for both) were added to the cells to check the effect of the peptides on the cells for 24 h. After 24 h, 100 µl (50 µg) of MTT substrate was added to the cells and the plate was continued to incubate for 3 h at 37 °C with 5% CO_2. Later the formazan crystals formed were dissolved in 100 µl of DMSO and the absorbance was measured at 570 nm in Multimode Micro plate reader (Synergy HIM).

RT-qPCR assay. The effect of gramicidin S and melittin was tested against the SARS-CoV-2 with different concentrations. Remdesivir was run as an assay control. The titers for the virus were adjusted such that there was only viral replication and no cytolysis. Briefly, the virus (MOI 0.1) was pre-incubated with different concentrations of gramicidin S and melittin (0.1–10 µg) for an hour at 37 °C. After the incubation, virus inoculum containing gramicidin S and melittin was added to the Vero cells in duplicates (50 µl/well). Remdesivir (1 µM) was added to the Vero cells without pre-incubation as in the case of peptides. All the experimental groups were left for infection for 3 h while maintaining at 37 °C with 5% CO_2. Post-infection (PI), media containing viral inoculum and the gramicidin S and melittin was removed and replaced with 200 µl of fresh DMEM media containing 10% FBS and the experimental groups were maintained for varying time points in an incubator maintained at 37 °C with 5% CO_2. Post-incubation, cell supernatants from the experimental groups were collected and spun for 10 min at 6000 g to remove debris and the supernatant was transferred to fresh collection tubes and later were processed to isolate viral RNA. RNA was extracted from 200 µL aliquots of sample supernatant using the MagMAX™ Viral/Pathogen Extraction Kit (Applied Biosystems, Thermofisher). Briefly, the viral supernatants from the test groups were added into the deep well plate (KingFisher™Thermo Scientific) along with a lysis buffer containing the following components—260 µL, MagMAX™ Viral/Pathogen Binding Solution; 10 µL, MVP-II Binding Beads; 5 µL, MagMAX™Viral/Pathogen Proteinase-K, for 200 µL of sample. (Extraction was performed using KingFisher Flex (version 1.01, Thermo Scientific) according to manufactures instructions). The eluted RNA was immediately stored in – 80 °C until further use.

The detection of SARS-CoV-2 was done using COVID-19 RT-PCR Detection Kit (Fosun 2019-nCoV qPCR, Shanghai Fosun Long March Medical Science Co. Ltd.) according to the manufacturer's instructions. The kit detects Envelope gene (E; ROX labelled), Nucleocapsid gene (N-JOE labelled) and Open Reading Frame1ab (ORF1ab, FAM labelled) specific to SARS-CoV-2 for detection and amplification of the cDNA. SARS-CoV-2 cDNA (Ct ~ 28) was used as a positive control. The log viral particles and a semi–log graph was plotted through the linear regression equation obtained using the RNA extracted from the known viral particles by RT-qPCR, using N- gene specific to SARS CoV-2 virus.

Immunocytochemistry. The Vero cells were seeded in 6-well plate with the sterile glass cover slips. Cells at 90–95% confluency were considered for SARS-CoV-2 infection. Briefly, gramicidin S and melittin, were pre-incubated with SARS-CoV-2 virus for 1 h at 37 °C with 1.5 µg/100 µl and 3 µg/100 µl respectively. Later, the viral inoculum incubated with peptides were used to infect Vero cells on the glass coverslips. After 3 h of infection, the viral inoculum containing the peptides was replaced with fresh media with 10% FBS until 12 and 24 h. Parallel controls were maintained without the drug treatment. After 12 and 24 h, the treated and untreated cells were fixed with 4% paraformaldehyde and processed further for immunocytochemistry. The fixed samples were washed thrice with PBS and the cells were permeabilized using 0.3% Triton X-100 (Sigma, cat. no.: X100; Lot no.: 056K0045) in PBS for 15 min at room temperature (RT). Then the cells were washed with PBS, thrice for 5 min each at RT. The cells were incubated with the 3% Bovine Serum Albumin (BSA) (Sigma) in PBS, for 1 h at RT to block the nonspecific antibody binding. Later the experimental groups were incubated with the anti-sera for RBD of SARS-CoV-2 (1:200) prepared in 1% BSA made in PBS (anti-sera against SARS-CoV-2 was raised in rabbits and validated using ELISA at CCMB) overnight at 4 °C. After incubation the cells were washed with PBST, thrice at RT for 10 min each. Later the cells were incubated with the secondary anti-Rabbit IgG antibody conjugated with Alexa Fluor 488 (Life Technologies, Cat. no.: A11008; Lot no.: 1735088) at the dilution of 1:200 in 1% BSA made in PBS. Rhodamine Phalloidin (Life Technologies, Cat. no.: R415; Lot no.: 1738179) was used to label F-actin. The cells were incubated with secondary antibody and Rhodamine phalloidin mix for 1 h at room temperature. After incubation the cells were washed with PBST, thrice at RT for 10 min each. Then, the cover slips containing the cells were mounted over the pre-cleaned slides using Vectashield mounting medium containing DAPI (for nuclear staining) (Vector Laboratories, Cat. no.: H-1200, Lot no.: ZC1216). Images were obtained using confocal microscope FV3000 with software version 2.4.1.198 (Olympus Life Sciences Solutions) in Light Scanning Microscopy (LSM) mode.

Proteomic analysis. Total protein was extracted from the control Vero cells, Vero cells infected with SARS-CoV-2 and Vero cells infected with SARS-CoV-2 and treated with gramicidin S and melittin separately. The cells were collected at 24 and 48 h independently. The samples were centrifuged and pellet was dissolved in protein solubilisation buffer[41,42] and sonicated for 10 min at BSL3 lab facility. The protein samples were further

centrifuged for 30 min at 14,000 RPM to remove the cell debris. Quantification of the pooled protein samples were performed using Amido Black method against BSA standard. A 200 µg of total protein from all the experimental groups were electrophoresed in 10% SDS-PAGE, Commassie R250 stained, destained and gel excised in to four fractions based on molecular weight. In-gel trypsin digestion and iTRAQ labeling and purification were performed as described earlier[42–44]. iTRAQ label was labelled as 114—Control; 115—Infection; 116—Infected cells treated with Melittin and 117—Infected cells treated with gramicidin S. All labelled peptides were pooled and purified by running through C18 column. Peptides were reconstituted in 5% acetonitrile (ACN) & 0.2% formic acid and then subjected to the Liquid Chromatography Mass Spectrometry (LCMS/MSMS) analysis in OrbitrapVelos Nano analyzer (Q-Exactive HF). The proteomic data obtained from the mass spectrometer were analysed against human proteome and SARS-CoV-2 proteome data. All the obtained proteome data were tabulated and differential expression in SARS-CoV-2 proteins were estimated against the control negative samples. The obtained proteome data was analysed for its heat map expression profile using heatmapper software[45] (www.heatmapper.ca). Network and pathway analysis of the associated proteins were performed using STRING v11.5[46] (https://string-db.org).

Molecular docking. The receptor binding domain (RBD) of the SARS-CoV-2 spike protein was obtained by editing the crystal structure of the C-terminal domain of the SARS-CoV-2 spike protein in complex with human ACE2 (PDB id: 6zlg)[47]. The ID of the structure used for gramicidin S monomer is CCDC 626343. Monomeric melittin structure was obtained by editing the crystal structure of tetrameric melittin (PDB id: 2mlt). The structures were generated using Discovery Studio v19.1.0.18287 (2019). Interactions between amino acids were visualized using LigPlot[28].

Statistical analysis. All the experiments were performed in duplicates with technical replicates (n = 6). The data analysis and graphs were generated using GraphPad Prism (*Ver* 8.4.2). All the values were represented as mean ± SD.

Ethics approval. The Anti-SARS CoV-2 study was approved from Institutional Bio-safety Committee of CSIR-Centre for Cellular and Molecular Biology, Hyderabad, India.

Received: 23 October 2021; Accepted: 16 February 2022
Published online: 02 March 2022

References

1. Chilamakuri, R. & Agarwal, S. COVID-19: Characteristics and therapeutics. *Cells* **10**, 206 (2021).
2. Creech, C. B., Walker, S. C. & Samuels, R. J. SARS-CoV-2 vaccines. *JAMA* **325**, 1318–1320 (2021).
3. Bok, K., Sitar, S., Graham, B. S. & Mascola, J. R. Accelerated COVID-19 vaccine development: Milestones, lessons, and prospects. *Immunity* **54**, 1636–1651 (2021).
4. Hacisuleyman, E. *et al.* Vaccine breakthrough infections with SARS-CoV-2 variants. *N. Engl. J. Med.* **384**, 2212–2218 (2021).
5. Taylor, P. C. *et al.* Neutralizing monoclonal antibodies for treatment of COVID-19. *Nat. Rev. Immunol.* **1**, 382–393 (2021).
6. Dittmar, M. *et al.* Drug repurposing screens reveal cell-type-specificentry pathways and FDA-approved drugs active against SARS-Cov-2. *Cell Rep.* **35**, 108959 (2021).
7. Gao, K., Nguyen, D. D., Chen, J., Wang, R. & Wei, G. Repositioning of 8565 existing drugs for COVID-19. *J. Phys. Chem. Lett.* **11**, 5373–5382 (2020).
8. Yan, V. C. & Muller, F. L. Why remdesivir failed: Preclinical assumptions overestimate the clinical efficacy of remdesivir for COVID-19 and ebola. *Antimicrob. Agents Chemother.* **65**, e01117-e1121 (2021).
9. Ledford, H. COVID antiviral pills: What scientists still want to know. *Nature* **599**, 358–359 (2021).
10. Hu, B., Guo, H., Zhou, P. & Shi, Z. L. Characteristics of SARS-CoV-2 and COVID-19. *Nat. Rev. Microbiol.* **19**, 141–154 (2021).
11. Sitaram, N. & Nagaraj, R. Interaction of antimicrobial peptides with biological and model membranes: Structural and charge requirements for activity. *Biochim. Biophys. Acta* **1462**, 29–54 (1999).
12. Mahlapuu, M., Björn, C. & Ekblom, J. Antimicrobial peptides as therapeutic agents: Opportunities and challenges. *Crit. Rev. Biotechnol.* **40**, 978–992 (2020).
13. Prenner, E. J., Lewis, R. N. A. H. & McElhaney, R. N. The interaction of the antimicrobial peptide gramicidin S with lipidbilayer model and biological membranes. *Biochem. Biophys. Acta.* **1462**, 201–221 (1999).
14. Raghuraman, H. & Chattopadhyay, A. Melittin: A membrane-active peptide with diversefunctions. *Biosci. Rep.* **27**, 189–223 (2007).
15. Tonk, M., Ružek, D. & Vilcinskas, A. Compelling evidence for the activity of antiviral peptides against SARS-CoV-2. *Viruses* **13**, 912 (2021).
16. Mahendran, A. S. K., Lim, Y. S., Fang, C.-M., Loh, H.-S. & Le, C. F. The potential of antiviral peptides as COVID-19 therapeutics. *Front. Pharmacol.* **11**, 575444 (2020).
17. Ghosh, S. K. & Weinberg, A. Ramping up antimicrobial peptides against severe acute respiratory syndrome coronavirus-2. *Front. Mol. Biosci.* **8**, 620806 (2021).
18. Memariani, H., Memariani, M., Moravvej, H. & Shahidi-Dadras, M. Melittin: A venom-derived peptide with promising anti-viral properties. *Eur. J. Clin. Microbiol. Infect. Dis.* **39**, 5–17 (2020).
19. Al-Rabia, M. W. *et al.* Repurposing of sitagliptin-melittin optimized nanoformula against sars-cov-2: Antiviral screening and molecular docking studies. *Pharmaceutics* **13**, 307 (2021).
20. Hossen, M., Gan, S. H. & Khalil, M. Melittin, a potential natural toxin of crude bee venom: probable future arsenal in the treatment of diabetes mellitus. *J. Chem.* **2017**, 1–10 (2017).
21. Duffy, C. *et al.* Honeybee venom and melittin suppress growth factor receptor activation in HER2-enriched and triple-negative breast cancer. *NPJ Precis. Oncol.* **4**, 24 (2020).
22. Berditsch, M., Lux, H., Babii, O., Afonin, S. & Ulrich, A. S. Therapeutic potential of GramicidinS in the treatment of root canal infections. *Pharmaceuticals* **9**, 56 (2016).
23. Hood, J. L., Jallouk, A. P., Campbell, N., Ratner, L. & Wickline, S. A. Cytolytic nanoparticles attenuate HIV-1 infectivity. *Antivir. Ther.* **18**, 95–103 (2013).
24. Uddin, M. B. *et al.* Inhibitory effects of bee venom and its components against viruses in vitro and in vivo. *J. Microbiol.* **54**, 853–866 (2016).

25. Swierstra, J., Kapoerchan, V., Knijnenburg, A., van Belkum, A. & Overhand, M. Structure, toxicity and antibiotic activity of gramicidin S and derivatives. *Eur. J. Clin. Microbiol. Infect. Dis.* **35**, 763–769 (2016).
26. Askari, P., Namaei, M. H., Ghazvini, K. & Hosseini, M. In vitro and in vivo toxicity and antibacterial efficacy of melittin against clinical extensively drug-resistant bacteria. *BMC Pharmacol. Toxicol.* **22**, 42 (2021).
27. Pierce, B. G. *et al.* ZDOCK server: Interactive docking prediction of protein-protein complexes and symmetric multimers. *Bioinformatics* **30**(12), 1771–1773 (2014).
28. Laskowski, R. A. & Swindells, M. B. LigPlot+: Multiple ligand-protein interaction diagrams for drug discovery. *J. Chem. Inf. Model.* **51**, 2778–2786 (2011).
29. Coleman, C. M. & Frieman, M. B. Coronaviruses: Important emerging human pathogens. *J. Virol.* **88**, 5209–5212 (2014).
30. Zhu, Z. *et al.* From SARS and MERS to COVID-a brief summary and comparison of severe acute respiratory infections caused by three highly pathogenic human corona viruses. *Respir. Res.* **21**, 224 (2020).
31. Idris, M. M., Banu, S., Siva, A. B. & Nagaraj, R. Down regulation of defensin genes in SARS-CoV-2 infection. *MedRxiV* https://doi.org/10.1101/2020.09.21.20195537 (2020).
32. Kasozi, K. I. *et al.* Bee venom: A potential complementary medicine candidate for SARS-CoV-2 infections. *Front. Public Health* **8**, 75 (2020).
33. Bansal, P., Kumar, R., Singh, J. & Dhanda, S. In silico molecular docking of SARS-CoV-2 surface proteins with microbial non-ribosomal peptides: Identification of potential drugs. *J. Proteins Proteom.* **1**, 1–8 (2021).
34. Huang, S. Y. Exploring the potential of global protein–protein docking: An overview and critical assessment of current programs for automatic ab initio docking. *Drug. Discov. Today* **20**, 969–977 (2015).
35. Juvvadi, P., Vunnam, S. & Merrifield, R. B. Synthetic melittin, its enantio, retro, and retroenantio isomers, and selected chimeric analogs: Their antibacterial, hemolytic, and lipid bilayer action. *J. Am. Chem. Soc.* **118**, 8989–8997 (1996).
36. Guan, Q. *et al.* Recent advances in the exploration of therapeutic analogues of gramicidin s, an old but still potent antimicrobial peptide. *J. Med. Chem.* **62**, 7603–7617 (2019).
37. Lv, S., Sylvestre, M., Song, K. & Pun, S. H. Development of D-melittin polymeric nanoparticles for anti-cancer treatment. *Biomaterials* **277**, 121076 (2021).
38. Krishnan, S. *et al.* Metabolic perturbation associated with COVID-19 disease severity and SARS-CoV-2 replication. *Mol. Cell Proteom.* https://doi.org/10.1101/2021.02.24.432759 (2021).
39. Bojkova, D. *et al.* Targeting pentosephosphate pathway for SARS-CoV-2 therapy. *Metabolites* **11**, 669 (2021).
40. Flynn, R. A. *et al.* Discovery and functional interrogation of SARS-CoV-2 RNA-host protein interactions. *Cell* **184**, 2394–2411 (2021).
41. Saxena, S. *et al.* Proteomic analysis of zebrafish caudal fin regeneration. *Mol. Cell. Proteom.* **111**, 014118 (2012).
42. Purushothaman, S. *et al.* Transcriptomic and proteomic analyses of *Amphiurafiliformis* arm tissue-undergoing regeneration. *J. Proteomics.* **112**, 113–124 (2015).
43. Nagumantri, S. P., Banu, S. & Idris, M. M. Transcriptomic and proteomic analysis of *Hemidactylusfrenatus* during initial stages of tail regeneration. *Sci Rep.* **11**, 3675 (2021).
44. Banu, S. *et al.* Understanding the complexity of Epimorphic Regeneration in zebrafish: A Transcriptomic and Proteomic approach. *BioRxiv.* **76**, 429 (2021).
45. Babicki, S. *et al.* Heatmapper: Web-enabled heat mapping for all. *Nucleic Acids Res.* **44**(W1), W147–W153 (2016).
46. Szklarczyk, D. *et al.* STRING v11: Protein-protein association networks with increased coverage, supporting functional discovery in genome-wide experimental datasets. *Nucleic Acids Res.* **47**, D607-613 (2019).
47. Wang, Q. *et al.* Structural and functional basis of SARS-CoV-2 entry by using human ACE2. *Cell* **181**, 894–904 (2020).

Acknowledgements

BKK would like to acknowledge financial support from Council of Scientific and Industrial Research (CSIR MLP0056). RN is Indian National Academy (INSA) Senior Scientist. The authors are thankful to Ms. Noorul Fowzia for critically reviewing the manuscript.

Author contributions

M.G.E., Y.P., S.B. and S.R.—Performed the experiment. M.G.E., Y.P., S.B., S.R., R.N., B.K. and M.M.I. analyzed the data. M.G.E., Y.P., S.B., R.N., B.K. and M.M.I. wrote the manuscript.

Competing interests

The authors declare no competing interests.

Additional information

Correspondence and requests for materials should be addressed to B.K.K. or M.M.I.

Reprints and permissions information is available at www.nature.com/reprints.

Publisher's note Springer Nature remains neutral with regard to jurisdictional claims in published maps and institutional affiliations.